Process Biochemistry 129 (2023) 185–199

Contents lists available at ScienceDirect

Process Biochemistry

journal homepage: www.elsevier.com/locate/procbio

Unrivalled insight into potential biopharmaceutical application of *Allardia tridactylites* (Kar. & Kir.) Sch. Bip.: Chemodiversity, *in vitro* bioactivities and computational analysis

Muhammad Imran Tousif [a], Mamona Nazir [b], Naheed Riaz [c], Muhammad Saleem [c,*], Main Habib Ur Rehman Mahmood [a], Muhammad Ahsan [a], Saba Tauseef [d], Nusrat Shafiq [e], Aniqa Moveed [e], Gokhan Zengin [f,*], Serdar Korpayev [g], Zaheer Abbas [h], Shabir Muhammad [i], Saleh S. Alarfaji [i]

[a] Department of Chemistry, Division of Science and Technology, University of Education, 54770 Lahore, Pakistan
[b] Department of Chemistry, Government Sadiq College Women University Bahawalpur, 63100 Bahawalpur, Pakistan
[c] Institute of Chemistry, Baghdad Campus the Islamia University of Bahawalpur, 63100 Bahawalpur, Pakistan
[d] Dr. Panjwani Center for Molecular Medicine and Drug Research, International Center for Chemical and Biological Sciences, University of Karachi, Karachi, Pakistan
[e] Synthetic and Natural product Discovery Lab., Department of Chemistry, Government College Women University Faisalabad 38000, Pakistan
[f] Department of Biology, Science Faculty, Selcuk University, Konya, Turkey
[g] Biotechnology Institute, Ankara University, 06135 Ankara, Turkey
[h] Department of Botany, Division of Science and Technology, University of Education, 54770 Lahore, Pakistan
[i] Department of Chemistry, College of Science, King Khalid University, P.O. Box 9004, Abha 61413, Saudi Arabia

ARTICLE INFO

Keywords:
Allardia tridactylites
Bioactive compounds
Antioxidant potential
Enzyme inhibition
Computational analyses

ABSTRACT

This research work offers unrivalled insight into the chemodiversity, antioxidant and enzyme inhibition activities of *Allardia tridactylites* substantiated by computational analysis. Flowers and leaves of *A. tridactylites* were extracted separately with hexane, chloroform, ethyl acetate and ethanol to prepare four extracts of each part. Highest antioxidant potential for the ATFA and ATFLA fractions was observed in the CUPRAC (cupric ion reducing antioxidant capacity) assay as 115.57 ± 1.16 and 112.79 ± 1.8 mg of trolox equivalents per gram of the extract (mg TE/g extract) respectively, followed by chloroform and ethyl acetate extracts of the leaves and the flowers. In tyrosinase inhibition assay, the ATFE was found most active (28.92 ± 1.42 mg of Kojic acid equivalents per gram of the extract (mg KAE/g extract), while against α-amylase and α-glucosidase, the ATLC (0.63 ± 0.02 mmol of acarbose equivalents per gram of the extract (mmol ACAE/g extract) and ATFH (1.10 ± 0.01 mmol ACAE/g) were the most active respectively. Overall, ATLA and ATFA were rich in phenolics and flavonoids and also exhibited higher antioxidant activities, while in enzyme inhibition assay, the low polar extracts were more active. UHPLC-MS analysis of crude ethanolic extract result in identification of 125 secondary metabolites of various classes. The findings from various multidirectional investigations indicated that this plant held significant importance for the biopharmaceutical industries, as it served as a valuable source for the development of multiple formulations that were effective in targeting major biological enzymes.

1. Introduction

Natural products have had a significant impact in drug development, and there are several ways in which they have contributed to drug development: e.g. Lead molecule identification: Many natural compounds have been identified as lead molecules for the development of new drugs. Paclitaxel, for example, is an anti-cancer drug that was discovered in the Pacific yew tree. Natural product modification: Natural products can be modified in the laboratory to improve their pharmacological properties, such as potency and selectivity. For example, azithromycin, a semi-synthetic derivative of the antibiotic erythromycin, has better pharmacokinetics and is more effective against certain bacterial infections [1]. *Allardia tridactylites* (Syn. *Waldheimia tridactylites*) a plant of Asteraceae family and locally known as "Tarqan" or

* Corresponding authors.
E-mail addresses: m.saleem@iub.edu.pk (M. Saleem), gokhanzengin@selcuk.edu.tr (G. Zengin).

https://doi.org/10.1016/j.procbio.2023.03.027
Received 3 February 2023; Received in revised form 21 March 2023; Accepted 23 March 2023
Available online 24 March 2023

"Patkanstwa" [2]. It is distributed in Pakistan, China, Afghanistan, Mongolia, Russia, Nepal, East and West Himalayas [3,4]. In Pakistan, it is found in Baltistan, Hunza, Chitral, Swat, Shangla, Deosai National Park (DNP) [2]. It is a perennial herbaceous plant and grows in the sandy gravels, rock crevices, talus on mountain slopes and on the fringe of streams in the alpine and sub-nival zones. It is found within the elevational range of 3200–5000 m above sea level in the lofty mountains of the Himalaya, the Karakorum and the Hindu Kush [3]. Plant is small (up to 6 cm) glabrous and rosette herbs growing from much branched rhizome. Shoots are mono cephalous and densely branched with sub-sessile and cuneate leaves [3]. Locally, the decoction of *A. tridactylites* is used against food poisoning [2], whereas, in the vast Himalayan region of Nepal, it is reported as a source of antioxidants [2]. Other species of *Allardia* genus also provide some support to traditional medicinal system. *Allardia* has been demonstrated to be an extremely valuable genus in the creation and utilization of medicinal herbal products, and it could potentially serve as a plentiful source of lead compounds for the development of novel therapeutic agents [5]. Literature search revealed that *A. glabra* has been used as antiviral drug to treat conditions like influenza cold, wounds, and also used against fever, and skin diseases and as antiseptic [5,6]. It is also used to treat normal health condition such as headache, joint pain and fever; because of its aromatic properties, it is also used by the local populations in religious rituals (incense) [7]. *A. glabra* constitutes α-bisabolol, valeranone, chamazulene, spathulenol, *β*-caryophyllene, and caryophyllene oxide, oxygenated sesquiterpenes, sesquiterpene hydrocarbons and oxygenated monoterpenes [6]. Flower decoction of *A.tomentosa*is used in digestive disorders [2]. Despite of medicinal importance of *Allardia* plants, *A. tridactylites* is an ignored herb, since no phytochemical or pharmacological work has ever been reported on this plant. Therefore, in the present study, we investigated this herb for its complete secondary metabolic picture and also unveiled its total bioactive contents, antioxidant and enzyme inhibition potential. Further, computational analysis and molecular modeling offered better picture to understand its mechanism of action and medicinal importance.

2. Experimental procedures

2.1. Collection and preparation of the plant material

A. tridactylites was collected from the Deosai National Park (DNP) formally known Deosai Plateau or Deosai Plains in the Trans-Himalayan region of Baltistan, northern Pakistan. It was found at different habitats like among gravels, moraines and boulders in the altitudinal range of 4000–4200 m above sea level. The identification of plant was done by Dr. Zaheer Abbas a taxonomist at Department of Botany, University of Education, Campus Dera Ghazi Khan. The identified specimen was assigned voucher number DNP42, properly labeled, stamped and stored in the scientific laboratory of Central Karakorum National Park (CKNP) Skardu Baltistan. The plant materials were properly collected in cloth sacks, prostrated on plastic mats and shade dried for 20 days for further biochemical investigations.

2.2. Extraction of the plant material

The dried plant material (flower 2 Kg and leaves 1 Kg) were ground into semi-powder and macerated with 2 litre of *n*-hexane, chloroform, ethyl acetate and ethanol for ten days and concentrated with rotatory evaporator to get respective extracts of flowers (ethanol; ATFA 55 mg, ethyl acetate; ATFE 27 mg, *n*-hexane; ATFH 25 mg and chloroform; ATFC 30 mg, and leaves (ethanol; ATLA 58 mg, ethyl acetate; ATLE 35 mg, *n*-hexane; ATLH 24 mg and chloroform; ATLC 36 mg).

2.3. Measurement of total bioactive contents

Total bioactive contents of various extracts of *A. tridactylites* were measured through Folin-Ciocalteu (FC) reagent method as reported previously [8,9]. Total phenolic contents values were calculated as mg of gallic acid equivalent per gram of the extract (mg GAE/g). The total flavonoids contents (TFC) were calculated as mg of rutin equivalent per gram of the extract (mg RE/g extract) [10,11].

2.4. Antioxidant assays

The antioxidant potential of all extract was assessed through reducing power (FRAP and CUPRAC), radical scavenging (DPPH and ABTS) assays and the phosphomolybdenum assay; their results were expressed as trolox equivalents (mg TE/g extract). Whereas metal chelating power assay was also used to calculated antioxidant activity and results were expressed as mg EDTAE/g extract [8]. All assays were performed in triplicates.

2.5. Enzyme inhibition studies

The enzyme inhibition potential of all the extracts against acetylcholinesterase (AChE) (mg of galantamine equivalent per gram of the extract), Butyrylcholinesterase (BChE) (mg GALAE/g extract), Tyrosinase (mg KAE/g extract), α-Amylase (mmol ACAE/g extract), α-Glucosidase (mmol ACAE/g extract) was assessed through in-vitro standard methods as reported previously [12–14]. All assays were performed in triplicates.

2.6. UHPLC-MS analysis

Chemical profiling of the ethanolic extracts (whole plant) was done through UHPLC-MS (ultra-high-performance liquid chromatography mass spectrometry) analysis. Sample was filtered with 0.22 μM Nylon syringe filter and diluted 10X with methanol. Agilent 1290 Infinity LC system coupled to Agilent 6520 Accurate-Mass Q-TOF mass spectrometer with dual ESI source. Column and Auto sampler temperature is maintaining at 25 and 4 °C respectively. Flowrate rate was 0.5 mL/min while solvents A is 0.1 % formic acid in water and solvent B is 0.1 % formic acid in Acetonitrile. Injection volume is 1.0 μL. METLIN database was used for the tentative identification of the secondary metabolites [15].

2.7. Statistical analysis

ANOVA (Tukey's test) was used to assess whether or not there were significant variations in the levels of extracts between groups. The Pearson correlation test was used to examine the relationship between total bioactive components and biological activities. The correlation analysis was performed by using Graph Pad 9.0. Additionally, Principal Component Analysis (PCA) was used to determine whether the tested extracts were similar or different. SIMCA (version 14.0) was used for the PCA analysis.

2.8. Molecular docking methodology

Protein structure for AChE enzyme (*PDB ID: 1EVE*), tyrosinase (PDB ID:2Y9X), BChE enzyme (PDB ID: 5nn0), α-amylase (PDB ID: 3BAJ) and α-glucosidase (PDB ID: 3TOP) was selected from RCSB protein data bank and then downloaded in PDB format [16,17]. After that the downloaded protein was opened into Discovery Studio Visualizer v20. 1. 0. 20298 (Accelrys). In docking protein structure remain rigid, therefore all water molecules were deleted to make protein structure flexible, all heteroatoms were removed. Binding sites were predicted by selecting the native inhibitor as ligand and then binding site sphere was generated into this site [18]. And for docking purpose all ligand groups were deleted. Moreover, polar hydrogens were added. The final structure was saved in PDB format. The protein was edited using AutoDock Tools (ADT), the polar hydrogen atoms were added to the amino acid residues,

Table 1
Total phenolic (TPC) and flavonoid (TFC) contents of *A. tridactylites*.

Extract	Plant Part	TPC (mg GAE/g extract)*	TFC (mg RE/g extract)*
Ethanol (ATFA)	Flower	29.73 ± 0.41^{b}	34.62 ± 0.08^{a}
Ethyl Acetate (ATFE)		17.25 ± 0.55^{d}	25.59 ± 0.16^{b}
Chloroform (ATFC)		19.72 ± 0.75 ^{cd}	9.37 ± 0.10^{e}
Hexane (ATFH)		14.37 ± 0.23^{e}	2.42 ± 0.08 ^{g}
Ethanol (ATLA)	Leaves	32.88 ± 1.50^{a}	25.44 ± 0.23^{b}
Ethyl Acetate (ATLE)		20.22 ± 0.58^{c}	19.96 ± 0.49^{c}
Chloroform (ATLC)		20.61 ± 0.77^{c}	16.19 ± 0.09^{d}
Hexane (ATLH)		14.01 ± 0.43^{e}	5.31 ± 0.20 ^{f}

TPC= Total Phenolic Contents, TFC= Total Flavonoid Contents, *Values expressed are means of three parallel results ± Standard Deviations of three parallel measurements. Different superscript letters (a-g) indicate significant differences in the tested extracts ($p < 0.05$).

all atoms were assign radii and AD4 type, kollman and Gasteiger charges were assigned to all atoms of the protein. Then the protein was converted into PDBQT file by Autodock Tools v.1.5.7. This PDBQT file was used as an input for the AUTOGRID program [19]. AUTOGRID performed a pre-calculated atomic affinity grid maps for each atom type in the ligand plus an electrostatics map and a separate desolvation map present in the substrate molecule taking the entire protein as the search space [20,21]. Flexible ligand docking was performed for each compound. Ligand and protein was docked employing AutoDock/Vina the strongest docked pose was analyzed in Pymol (Schodinger). The results were shown using Discovery Studio Visualizer v20.1.0.20298 [22]. All chemical structures were drawn in ChemDraw 19.1 (Cambrigde Soft). After that three-dimensional structures were obtained in Chem3D 19.1. Each structure then was executed by applying MM2 and MMFF94 force field for energy minimization and molecular dynamics [23] Geometry optimization of the lowest energy conformer accomplished by density functional theory methods (DFT) at the B3LYP/6–311G* level., finally structure was saved as PDB format and converted into PDBQT format by using Open Babel, as it was requirement of AutoDock Vina docking [24] Then by using AutoDock Tools v. 1.5.7, ligand was detected by choose root and detect root all the Kollman and Gastieger charges were added by assigning AD4 type atomic radii [25].

3. Results and discussion

The collected plant of *A. tridactylites* was divided into two parts i.e flowers (ATF) and leaves (ATL). Both the plant parts were further divided each into four sub-parts and were extracted separately with ethanol, ethyl acetate, chloroform and hexane, and the obtained respective extracts were coded as flowers: ethanol (ATFA), ethyl acetate (ATFE), chloroform (ATFC)and hexane (ATFH), and leaves: ethanol (ATLA), ethyl acetate (ATLE), chloroform (ATLC) and hexane (ATLH). All the extracts were then studied for their total bioactive contents, antioxidant and enzyme inhibition potentials (Tables 1–3).

3.1. Total bioactive contents of *A. tridactylites*

All the extracts of *A. tridactylites* were analyzed for their total phenolic (TPC) and flavonoid (TFC) contents. The results indicated that almost all the extracts contain significant amount of phenolics and flavonoids, however, ATLA showed highest phenolic contents (32.88 ± 1.50 mg GAE/g extract) followed by ATFA (29.73 ± 0.41 mg GAE/g extract), while ATFH and ATLH were the weakest carriers of phenolic compounds. Almost similar trend was observed in case of TFC measurement, where ATFA and ATLA exhibited the contents as 34.62 ± 0.08 and 25.44 ± 0.23 mg RE/g extract, respectively, whereas, lowest contents were observed in hexane extracts (ATFH and ATLH). Other extracts, however, discloses varying degree of TPC and TFC contents (Table 1) depending upon the polarity of the extracting solvents. Overall these results prompted us to conclude that the whole plant of *A. tridactylites* is rich in bioactive contents with highest phenolic contents in leaves, while highest flavonoid contents were found in flower extracts, and most of these components were extracted in polar solvents like ethanol. It is further stated that ethanolis usually used to prepare

Table 2
Antioxidant activities of the extracts of *A. tridactylites*.

Extract	Plant Part	DPPH (mg TE/g extract)*	ABTS (mg TE/g extract)*	CUPRAC (mg TE/g extract)*	FRAP (mg TE/g extract)*	Phosphomolybdenum (mmol TE/g extract)*	Metal Chelating (mg EDTAE/g extract)*
Ethanol (ATFA)	Flowers	48.63 ± 0.10^{a}	94.68 ± 0.31^{b}	115.57 ± 1.16^{a}	72.25 ± 1.93^{b}	1.32 ± 0.03^{e}	16.01 ± 1.74 ^{cd}
Ethyl acetate (ATFE)		25.79 ± 0.17^{b}	70.29 ± 0.89^{c}	59.97 ± 1.01^{b}	42.12 ± 0.07^{c}	1.73 ± 0.04 ^{cd}	14.23 ± 0.23^{d}
Chloroform (ATFC)		2.99 ± 0.30^{d}	34.25 ± 0.32^{e}	53.09 ± 0.72^{d}	23.95 ± 0.23^{e}	1.80 ± 0.02^{bc}	6.10 ± 1.45^{e}
Hexane (ATFH)		NA	14.66 ± 0.50 ^{f}	46.34 ± 0.51^{e}	20.56 ± 0.44 ^{f}	2.35 ± 0.09^{a}	24.46 ± 0.69^{a}
Ethanol (ATLA)	Leaves	48.75 ± 0.05^{a}	102.98 ± 0.13^{a}	112.79 ± 1.8^{a}	80.41 ± 0.27^{a}	1.27 ± 0.06^{e}	21.44 ± 0.71^{ab}
Ethyl acetate (ATLE)		10.84 ± 0.66^{c}	45.79 ± 1.2^{d}	55.01 ± 1.34 ^{cd}	33.01 ± 0.15^{d}	1.57 ± 0.07^{d}	14.82 ± 0.36^{d}
Chloroform (ATLC)		2.29 ± 0.26^{d}	34.84 ± 1.6^{e}	58.08 ± 0.20^{bc}	24.96 ± 0.89^{e}	1.77 ± 0.05 ^{cd}	18.69 ± 0.10^{bc}
Hexane (ATLH)		NA	15.21 ± 0.36 ^{f}	42.72 ± 1.09^{e}	16.50 ± 0.30 ^{g}	2.03 ± 0.09^{b}	23.59 ± 0.69^{a}

NA= not active, *Values expressed are means of three parallel results ± Standard Deviations of three parallel measurements. Different superscript letters (a-g) indicate significant differences in the tested extracts ($p < 0.05$).

Table 3
Enzyme Inhibition activities of the extracts of *A. tridactylites*.

Extract	Plant Part	AChE inhibition (mg GALAE/g extract)a	BChE inhibition (mg GALAE/g extract)a	Tyrosinase inhibition (mg KAE/g extract)a	α-Amylase inhibition (mmol ACAE/g extract)a	σ-Glucosidase inhibition (mmol ACAE/g extract)a
Ethanol (ATFA)	Flowers	3.72 ± 0.13^{bc}	0.82 ± 0.02^{d}	24.46 ± 0.52^{ab}	0.38 ± 0.01^{e}	0.23 ± 0.03^{b}
Ethyl Acetate (ATFE)		3.73 ± 011^{bc}	1.11 ± 0.13^{d}	28.92 ± 1.42^{a}	0.46 ± 0.01^{d}	1.05 ± 0.05^{a}
Chloroform (ATFC)		4.76 ± 0.16^{a}	2.92 ± 0.26^{b}	26.44 ± 2.43^{a}	0.61 ± 0.01^{ab}	1.04 ± 0.04^{a}
Hexane (ATFH)		4.06 ± 0.04^{b}	3.53 ± 0.19^{ab}	25.66 ± 1.32^{a}	0.58 ± 0.01^{ab}	1.10 ± 0.01^{a}
Ethanol (ATLA)	Leaves	3.29 ± 0.25^{c}	0.63 ± 0.08^{d}	17.12 ± 3.68^{b}	0.36 ± 0.01^{e}	0.02 ± 0.00^{c}
Ethyl acetate (ATLE)		3.57 ± 0.17^{bc}	1.90 ± 0.11^{c}	23.50 ± 1.60^{ab}	0.51 ± 0.01^{c}	0.94 ± 0.12^{a}
Chloroform (ATLC)		3.96 ± 0.15^{b}	2.89 ± 0.17^{b}	22.48 ± 3.30^{ab}	0.63 ± 0.02^{a}	1.03 ± 0.03^{a}
Hexane (ATLH)		3.89 ± 0.20^{b}	3.91 ± 0.37^{a}	25.64 ± 2.74^{a}	0.58 ± 0.02^{b}	1.07 ± 0.01^{a}

[a] Values expressed are means of three parallel results ± Standard Deviations of three parallel measurements. Different superscript letters (a-e) indicate significant differences in the tested extracts ($p < 0.05$).

tinctures of plant extracts, and it extracts large number of secondary metabolites, especially the phenolics; this fact substantiated our results.

3.2. Antioxidant activities

3.2.1. DPPH and ABTS free radical scavenging activities

Free radical scavenging activities of a plant extract are mostly associated with their phenolic and flavonoid contents; that the extracts with higher TPC and TFC exhibit higher radical scavenging activities [26]. Same trend was observed in the present study where the flower and leaf extracts of *A. tridactylites*, rich in phenolics and flavonoids, showed higher free radical scavenging activities (Table 2). ATLA and ATFA exhibited the most potent inhibition against ABTS free radical with values of 102.98 ± 0.13 and 94.68 ± 0.31 mg TE/g of the extract, respectively with the next higher values were associated with ATFE (70.29 ± 0.89 mg TE/g extract) and ATLE (45.79 ± 1.2 mg TE/g extract). Similar activity trend was observed against DPPH free radical, ATFA and ATLA were almost equally active (48 mg TE/g extract), followed by the activities of ATFE and ATLE, respectively (Table 2). The ATFH and ATLH extracts were found inactive against DPPH radical, and exhibited poor inhibition of ABTS free radicals (Table 2), it substantiated that phenolic and flavonoid rich plant extracts are potent free radical inhibitors.

3.2.2. Metal ion reducing power activities

Theoretically a good antioxidant must be a good metal reductant, thus the metal reducing power of phytochemicals is widely used to evaluate the antioxidant activity of plant extracts, which are rich in bioactive chemicals and possess potent electron-donating abilities and thus act as antioxidants [27]. In the present study, all the extracts of leaves and flowers of *A. tridactylites* were evaluated for their metal ion reducing power. ATFA and ATLA showed the highest reducing potential in CUPRAC assay with the values of 115.57 ± 1.16 and 112.79 ± 1.8 mg TE/g of the extract, respectively; whereas, ethyl acetate and chloroform extracts of leaves (ATLE and ATLC) and flowers (ATFE and ATFC) exhibited nearly equal activity (>55 mg TE/g of the extract Table 2), which indicated that in addition to phenolic and flavonoid, other metabolites are also imparting to the reducing power of the extracts. Almost same trend was observed in FRAP assay, where ATLA was the most active extract (80.41 ± 0.27 mg TE/g extract), followed by ATFA (72.25 ± 1.93 mg TE/g extract), and ATLE and ATFE were next in line (Table 2). Overall, the assays revealed that the extracts of *A. tridactylites* possessed significant antioxidant activity.

3.2.3. Total antioxidant activity

Total antioxidant activities of all the extracts were measured through Phospho-molybdenum assay. Interestingly, low polar hexane extracts were equally active from both the sources (ATFH: 2.35 ± 0.09 and ATLH: 2.03 ± 0.09 mmol TE/g extract), while ATFA and ATLA were least active in this assay (Table 2). Since, in this assay, the next active extracts were of chloroform i.e. ATFC (1.80 ± 0.02 mmol TE/g extract) and ATLC (1.77 ± 0.05 mmol TE/g extract), it is concluded that secondary metabolites (terpenoid, steroids and their glycosides) other than phenolics, probably the low polar components are also contributing to the antioxidant potential of *A. tridactylites*. Literature reports revealed that other than phenolics and flavonoids, terpenoids [28] and carboxylic acids [29] also contribute to metal reducing and chelating activities, thus, antioxidant potential of chloroform and hexane extracts could be attributed to the presence of relatively low polar terpenoids and or fatty acids/carboxylic acids.

3.2.4. Metal-chelating activities

Metal-chelation therapy is the administration of chelating agents to remove heavy metals from the body to minimize toxic effects, and it is also an established fact that metal chelators are as good antioxidants [30]. In metal chelating assay, the low polar extracts of flowers (ATFH) and leaves (ATLH) displayed highest values 24.46 ± 0.69 and 23.59 ± 0.69 mg EDTAE/g of the extract, respectively; however, ATLA also exhibited comparable metal-chelating activity with the value of 21.44 ± 0.71 mg EDTAE/g of the extract. In case of flower extracts, ATFC was least active, while in case of leave extracts, ATLE showed weakest activity (Table 2). These results also substantiate the role of low polar components including terpenoids and carboxylic acid analogs as potential antioxidant compounds [31].

3.3. Enzyme inhibition activities

All the extracts of flowers and leaves of *A. tridactylites* were further evaluated for their enzyme inhibition activities against acetylcholinesterase (AChE), butyrylcholinesterase (BChE), tyrosinase, α-amylase and α -glucosidase;the results are presented in Table 3.

3.3.1. AChE and BChE inhibitory activities of the extracts of A. tridactylites

To evaluate theanti-Alzheimer's properties of *A. tridactylites*, all the extracts from flowers and leaves were tested against AChE and BChE enzymes, which showed almost equal inhibitory potential against AChE with the values in the range of 3.29 ± 0.25–4.76 ± 0.16 mg GALAE/g of the extract, with highest potential was observed for ATFC (4.76 ± 0.16 mg GALAE/g extract), ATFH (4.06 ± 0.04 mg GALAE/g extract) and ATLC (3.96 ± 0.15 mg GALAE/g extract). Other extracts also exhibited significant activity with slight differences (Table 3), which indicated that AChE inhibitory activity is attributed to combined effect of various secondary metabolites (terpenoid, steroids and their glycosides) in these extracts. However, against BChE enzyme, the hexane extract of leaves (ATLH) was the most active followed by hexane extract of flowers (ATFH) with the inhibitory values as 3.91 ± 0.37 and 3.53 ± 0.19 mg GALAE/g of the extract, respectively. The next most active fraction was chloroform extracts from both the sources, while ethanolic extracts were least active (Table 3). These observations revealed that for BChE inhibition, phenolics do not play a significant role, but other metabolites might be best binding with the enzyme. It is therefore, deduced that computational study could be the good idea to determine the active principals in these extracts.

3.3.2. Tyrosinase inhibitory activity of the extracts of A. tridactylites

Tyrosinase is a copper-containing oxidase enzyme with multifunctional properties. It plays a crucial role in catalyzing melanogenesis, which leads to the formation of melanin pigments in human skin. Additionally, tyrosinase also catalyzes browning reactions in fungi and damaged fruits, both of which are undesirable. Therefore, the use of potent tyrosinase inhibitors can help control these processes. Therefore, searching new tyrosinase inhibitors for use in food and cosmetic industry is an attractive area of research [32]. Currently available synthetic tyrosinase inhibitors induce toxic effects, and usually lack of efficacy, therefore, there is a dire need to search for safer natural inhibitors of tyrosinase, which are expected to be free of harmful side effects. New studies suggest the use of raw extracts of plants in formulations for the prevention or treatment of various human diseases [33]. In this quest, we evaluated all the extracts of flowers and leaves of *A. tridactylites* against tyrosinase, which showed nearly equal inhibitory potential (28.92 ± 1.42–17.12 ± 3.68 mg KAE/g extract) with highest value was attested for ATFE, and least was observed for ATLA (Table 3). The ATFH and ATLH showed equal inhibition (25.6 mg KAE/g extract) of tyrosinase, while other fractions also exhibited comparable and significant tyrosinase inhibitory potential (Table 3). These results suggest that the extract of *A. tridactylites* can be potential candidate in preparing conventional skin whitening formulations in cosmetic industry or anti-browning agents in food industry [34]. It is further deduced that along with phenolics, other compounds also impart to the anti-tyrosinase activity.

Table 4
the UHPLC-MS analysis of ethanolic extract whole plant (flower and leaves).

Sr. No.	Analyte Peak Name	Retention Time	Area / Height	Compound Name	Formula	M. Mass	Class
1	305.0572 (M+K+)	1.50	4.91	Methoxyvone	$C_{17}H_{14}O_3$	266.2960	Flavonoid
2	317.0928	1.49	3.76	Ginnalin B	$C_{13}H_{16}O_9$	316.2620	phenolic
3	429.2146	1.49	4.87	Taraxacolide 1-O-β-D-glucopyranoside	$C_{21}H_{32}O_9$	428.4780	Phenolic
4	439.1663	1.53	4.12	Broussonol D	$C_{25}H_{26}O_7$	438.1679	Flavonoid
5	321.1113	1.73	6.93	Erythrinin A	$C_{20}H_{16}O_4$	320.1049	Flavonoid
6	190.0897	1.68	5.79	Indole-3-methyl acetate	$C_{11}H_{11}NO_2$	189.0790	Alkaloid
7	343.0882	1.74	6.24	8-Hydroxygalangin 7-methyl ether 8-acetate	$C_{18}H_{14}O_7$	342.0740	Flavonoid
8	311.1117 (M+H+)	2.74	13.27	(E)− 1-O-Cinnamoyl-β-D-glucose	$C_{15}H_{18}O_7$	310.1053	Phenolic
9	326.1012	2.97	7.23	Avenanthramide L	$C_{18}H_{15}NO_5$	325.0950	Phenolic
10	373.1664 (M+NH4 +)	3.12	9.43	Tetrahydrocurcumin	$C_{21}H_{24}O_6$	372.1573	Phenolic
11	291.064 (M+K+)	3.41	9.31	Methyl 3,4,5-trimethoxycinnamate	$C_{13}H_{16}O_5$	252.0998	Phenolic
12	288.0868	3.86	5.27	Citrusinine II	$C_{15}H_{13}NO_5$	287.0794	acridones
13	251.1289	4.06	7.24	Helinorbisabone	$C_{14}H_{18}O_4$	250.1205	Phenolic
14	414.1529	4.36	5.40	(±)-α-Narcotine	$C_{22}H_{23}NO_7$	413.1475	Alkaloid
15	286.1437	4.46	5.87	(-)-Morphine	$C_{17}H_{19}NO_3$	285.1365	Alkaloid
16	360.1805 (M+CH3OH+H+)	4.53	4.88	6-Monoacetylmorphine	$C_{19}H_{21}NO_4$	327.1471	Alkaloid
17	360.1891 (M+NH4 +)	4.53	5.06	Brosimacutin C	$C_{20}H_{22}O_5$	342.1467	Flavonoid
18	378.1909 (M+CH3OH+H+)	4.55	3.78	Aknadicine	$C_{19}H_{23}NO_5$	345.1576	Alkaloid
19	261.1105 (M+Na+)	4.68	6.94	1-(3-Ethyl-2,4-dihydroxy-6-methoxyphenyl)− 1-butanone	$C_{13}H_{18}O_4$	238.1205	Phenolic
20	416.1874 (M+NH4$^+$)	4.75	6.80	Methyl 3,4-dihydroxy-5-prenylbenzoate 3-glucoside	$C_{19}H_{26}O_9$	398.1577	Phenolic
21	463.1309	4.87	4.60	Isorhamnetin 7-rhamnoside	$C_{22}H_{22}O_{11}$	462.1162	Flavonoid
22	338.1276	4.83	5.38	1 H-Indol-3-ylacetyl-myo-inositol	$C_{16}H_{19}NO_7$	337.1162	Alkaloid
23	347.0505	4.85	3.10	3,3'-Bisjuglone	$C_{20}H_{10}O_6$	346.2940	Phenolic
24	289.1048	4.94	9.11	2',4',α-Trihydroxy-4-methoxydihydrochalcone	$C_{16}H_{16}O_5$	288.0998	Flavonoid
25	395.1284 (M+Na+)	5.02	5.89	Citrusin E	$C_{17}H_{24}O_9$	372.3700	Flavonoid
26	549.2671	5.04	3.66	Archangelolide	$C_{29}H_{40}O_{10}$	548.2621	Terpenoid
27	323.1638	5.24	4.72	Derricin	$C_{21}H_{22}O_3$	322.4040	Phenolic
28	364.1882	5.23	4.21	Dioncophylline C	$C_{23}H_{25}NO_3$	534.2829	Alkaloid
29	452.2076	5.28	6.98	Piscerythramine	$C_{26}H_{29}NO_6$	451.1994	Flavonoid
30	386.1968	5.18	4.09	Thalicpureine	$C_{22}H_{27}NO_5$	385.1889	Phenolic
31	439.1315	5.32	4.29	Villinol	$C_{24}H_{22}O_8$	438.4320	Phenolic
32	319.0936	5.35	10.65	Musanolone F	$C_{20}H_{14}O_4$	318.3280	Phenolic
33	411.1374	5.52	4.02	(5α,6α,8α,11α)− 8-Hydroxy-2-oxo-1(10),3-guaiadien-12,6-olide-15-al 8-(4-hydroxyphenylacetate)	$C_{23}H_{22}O_7$	410.1365	Phenolic
34	400.1726	5.82	5.63	Glaudine	$C_{22}H_{25}NO_6$	399.1681	Alkaloid
35	408.2128	5.89	7.07	Ancistrocladine	$C_{25}H_{29}NO_4$	408.2169	Alkaloid
36	419.2424	5.87	7.62	Phyllanthin	$C_{24}H_{34}O_6$	418.2355	Phenolic
37	243.1009	6.03	5.73	2',4'-Dihydroxydihydrochalcone	$C_{15}H_{14}O_3$	242.2740	Flavonoid
38	439.2165	5.96	6.06	Deacetoxy-7-Oxogedunin	$C_{26}H_{30}O_6$	438.5200	limonoid
39	481.2350 (M+Na+)	6.17	4.90	Sophoradochromene	$C_{30}H_{34}O_4$	458.5980	Phenolic
40	507.3096	6.29	4.63	Mucronine A	$C_{29}H_{38}N_4O_4$	506.6470	Alkaloid
41	651.3336	6.32	6.25	Thapsigargin	$C_{34}H_{50}O_{12}$	650.7620	Terpenoid
42	325.1633	6.34	8.40	Chamissonolide	$C_{17}H_{24}O_6$	324.3730	Terpenoid
43	521.3258	6.35	5.30	24,25-Diacetylvulgaroside	$C_{29}H_{44}O_8$	520.6630	Terpenoid
44	293.1751	6.43	4.48	9-Acetoxyfukinanolide	$C_{17}H_{24}O_4$	292.3750	terpenoid
45	551.3178 (M+CH3OH+H+)	6.47	6.41	Corchoroside B	$C_{29}H_{42}O_8$	518.6470	steroidal glycosides
46	364.1879	6.59	4.33	Dioncophylline C	$C_{23}H_{25}NO_3$	363.4570	Alkaloid
47	374.2325 (M+NH4$^+$)	6.65	4.96	Estradiol Diacetate	$C_{22}H_{28}O_4$	356.4620	Steroid
48	597.2793 (M+Na+)	6.68	6.10	Herbimycin	$C_{30}H_{42}N_2O_9$	574.6710	Alkaloid
49	458.2536 (M+NH4 +)	6.85	7.75	Deacetylgedunin	$C_{26}H_{32}O_6$	440.5360	Terpenoid
50	603.1752	6.68	4.41	Amaroswerin	$C_{29}H_{30}O_{14}$	602.5450	Phenolic
51	402.2625 (M+NH4 +)	6.74	5.46	3,12-Dioxochola-4,6-dien-24-oic Acid	$C_{24}H_{32}O_4$	384.5160	Steroid
52	402.2446 (M+NH4 +)	6.73	7.70	Cinnzeylanol	$C_{20}H_{32}O_7$	384.4690	Terpenoid
53	409.1806 (M+CH3OH+H+)	6.78	10.41	(3 S)− 7-hydroxy-2',3',4',5',8-pentamethoxyisoflavan	$C_{20}H_{24}O_7$	376.4050	Flavonoid
54	652.3993 (M+NH4 +)	6.79	4.91	Pandaroside B	$C_{35}H_{54}O_{10}$	634.8070	Steroid
55	455.0687 (M+Na+)	6.69	3.15	Kaempferol 3-*p*-coumarate	$C_{24}H_{16}O_8$	432.3840	Phenolic
56	490.3135 (M+CH3OH+H+)	6.79	4.44	N-docosahexaenoyl glutamic acid	$C_{27}H_{39}NO_5$	457.2828	Phyto
57	368.2044 (M+NH4 +)	6.86	5.70	strychnine N-oxide	C21H22N2O3	350.1630	Alkaloids
58	353.1578	6.85	11.17	Coriandrone D	$C_{18}H_{24}O_7$	352.3830	Phenolic

(*continued on next page*)

Table 4 (*continued*)

Sr. No.	Analyte Peak Name	Retention Time	Area / Height	Compound Name	Formula	M. Mass	Class
59	459.2734	6.85	4.87	Lucidenic acid A	$C_{27}H_{38}O_6$	458.5950	Triterpenoid
60	446.2880 (M+NH4 +)	6.90	6.75	2-Angeloyl-9-(3-methyl-2E-pentenoyl)− 2β,9α-dihydroxy-4Z,10(14)-oplopadien-3-one	$C_{26}H_{36}O_5$	428.5690	Terpenoid
61	359.1440 (M+Na+)	6.89	5.60	Nb-Feruloyltryptamine	$C_{20}H_{20}N_2O_3$	336.3910	Phenolic
62	666.3595	6.90	7.87	Jubanine C	$C_{39}H_{47}N_5O_5$	665.8350	Oligopeptides
63	337.1395	6.92	4.77	Semilepidinoside A	$C_{16}H_{20}N_2O_6$	336.3440	Glycoside
64	384.1988 (M+NH4 +)	6.98	10.08	4-Acetyl-2-prenylphenol glucoside	$C_{19}H_{26}O_7$	366.4100	Phenolic
65							
66	479.2381 (M+Na+)	7.02	15.70	Lucidenolactone	$C_{27}H_{36}O_6$	456.2512	Triterpenoid
67	502.2781 (M+NH4 +)	7.01	6.72	Dihydrogedunin	$C_{28}H_{36}O_7$	484.2461	limonoid
68	291.1589	6.94	6.76	[6]-Dehydrogingerdione	$C_{17}H_{22}O_4$	290.1518	Phenolic
69	349.1023	6.97	5.25	Calopogoniumisoflavone B	$C_{21}H_{16}O_5$	348.0998	Flavonoid
70	412.2285	7.03	6.27	Lasiocarpine	$C_{21}H_{33}NO_7$	411.2257	alkaloid
71	412.2470 (M+NH4 +)	7.05	3.71	Gancaonin J	$C_{25}H_{30}O_4$	394.2144	Phenolic
72	803.3516 (M+K+)	7.03	5.56	Spinacoside D	$C_{40}H_{60}O_{14}$	764.3983	Triterpenoid saponin
73	398.2316 (M+NH4 +)	7.06	6.09	Chlorophorin	$C_{24}H_{28}O_4$	380.1988	Phenolic
74	357.2145	7.08	9.83	Piperochromanoic acid	$C_{22}H_{28}O_4$	356.1988	monoterpenoids
75	381.1882	7.07	7.22	Chaparrin	$C_{20}H_{28}O_7$	380.1835	Triterpenoid
76	377.1905 (M+Na+)	7.25	6.46	Pseudoyohimbine	$C_{21}H_{26}N_2O_3$	354.1943	Alkaloid
77	372.2342 (M+NH4 +)	7.05	6.26	Corynanthine	$C_{21}H_{26}N_2O_3$	354.1943	Alkaloid
78	414.2444 (M+NH4 +)	7.10	4.90	Echitovenine	$C_{23}H_{28}N_2O_4$	396.2049	Alkaloid
79	623.1850	7.12	3.46	Dioonflavone	$C_{36}H_{30}O_{10}$	622.1839	Flavonoid
80	289.1197	7.16	6.33	3-Carboxy-2,3,4,9-tetrahydro-1 H-pyrido [3,4-*b*] indole-1-propanoic acid	$C_{15}H_{16}N_2O_4$	288.1110	Alkaloid
81	439.2274 (M+CH3OH+H+)	7.23	6.77	Isomontanolide	$C_{22}H_{30}O_7$	406.1992	Sesquiterpene lactone
82	579.1419	7.18	2.22	Terniflorin	$C_{30}H_{26}O_{12}$	578.1424	Flavonoid glycoside
83	375.1749 (M+Na+)	7.15	5.66	[4]-Gingerdiol 3,5-diacetate	$C_{19}H_{28}O_6$	352.1886	Phenolic
84	415.2333	7.23	8.19	Deacetylvindoline	$C_{23}H_{30}N_2O_5$	414.2155	Alkaloid
85	648.3130	7.23	8.14	Beiwutine	$C_{33}H_{45}NO_{12}$	647.2942	Alkaloid
86	551.2336	7.22	4.54	Lappaol B	$C_{31}H_{34}O_9$	550.2203	Phenolic
87	548.3353 (M+NH4 +)	7.26	4.84	Kukoamine B	$C_{28}H_{42}N_4O_6$	530.3104	Alkaloid
88	513.1444	7.24	4.76	Emodinanthranol	$C_{30}H_{24}O_8$	512.1471	anthracenones
89	500.2796	7.30	4.96	Aconine	$C_{25}H_{41}NO_9$	499.2781	Alkaloid
90	414.2443 (M+NH4 +)	7.33	6.37	Isopetasoside	$C_{21}H_{32}O_7$	396.2148	Terpenoid
91	665.3643 (M+CH3OH+H+)	7.26	8.58	Tetrahydrogambogic Acid	$C_{38}H_{48}O_8$	632.3349	Pyranoxanthones
92	284.1639 (M+NH4 +)	7.45	4.07	Magnolol	$C_{18}H_{18}O_2$	266.1307	lignan
93	555.2642	7.45	4.36	Toonacilin	$C_{31}H_{38}O_9$	554.2516	sesquiterpenoid
94	279.1013	7.50	5.46	Ovalitenin A	$C_{18}H_{14}O_3$	278.0943	chalcones
95	295.1327	7.55	5.66	Eupomatenoid 5	$C_{19}H_{18}O_3$	294.1256	neolignan
96	546.3196	7.72	7.77	Americine	$C_{31}H_{39}N_5O_4$	545.3002	Phyto
97	551.2768	7.73	7.45	Aspecioside	$C_{29}H_{42}O_{10}$	550.2778	Phyto
98	695.3930	7.73	7.98	Capsoside A	$C_{33}H_{58}O_{15}$	694.3776	Glycoside
99	592.3593 (M+NH4 +)	7.76	6.57	Cucurbitacin A	$C_{32}H_{46}O_9$	574.3142	triterpenes
100	985.4347	7.84	4.97	Basellasaponin C	$C_{47}H_{68}O_{22}$	984.4202	Triterpenoid saponin
101	332.2057 (M+2H2 +)	7.98	11.16	cimicifoetiside A	$C_{37}H_{58}O_{10}$	662.4030	Triterpenoid glycosides
102	449.1518	7.95	5.43	Agehoustin C	$C_{22}H_{24}O_{10}$	448.1369	Flavonoid
103	713.3801 (M+Na+)	8.04	11.53	Gabunamine	$C_{42}H_{50}N_4O_5$	690.3781	Alkaloid
104	623.3728	7.98	6.11	3-O-Protocatechuoylceanothic acid	$C_{37}H_{50}O_8$	622.3506	Triterpenoid
105	773.4352 (M+Na+)	8.18	6.42	α-Hederin	$C_{41}H_{66}O_{12}$	750.4554	Triterpenoid saponin
107	770.4671 (M+NH4 +)	8.18	5.83	Polypodoside C	$C_{40}H_{64}O_{13}$	752.4347	Steroidal saponin
108	773.4154 (M+Na+)	8.18	6.79	Aginoside progenin	$C_{39}H_{64}O_{15}$	772.4245	Steroidal saponin
109	453.3333	8.25	6.51	3-Oxoursan (28–13)Olide	$C_{30}H_{44}O_3$	452.3290	Triterpenoid
110	817.4402 (M+Na+)	8.23	6.12	Rubbeloside A	$C_{42}H_{66}O_{14}$	794.4452	Phyto
111	398.2258	8.23	6.54	Echimidine	$C_{20}H_{31}NO_7$	397.2101	Alkaloid
112	814.4891(M+NH4 +)	8.23	6.00	Saponin E	$C_{42}H_{68}O_{14}$	796.4609	Saponin
113	813.4895 (M+CH3OH+H+)	8.23	6.72	Acutoside A	$C_{42}H_{68}O_{13}$	780.4660	Triterpenoid

(*continued on next page*)

Table 4 (*continued*)

Sr. No.	Analyte Peak Name	Retention Time	Area / Height	Compound Name	Formula	M. Mass	Class
114	301.0489	9.00	5.60	Mumefural	$C_{12}H_{12}O_9$	300.0481	Phyto
115	433.1563	9.09	5.19	7-Hydroxy-3',4'-methylenedioxyflavan 7-O-β-D-glucopyranoside	$C_{22}H_{24}O_9$	432.1420	Flavonoid
116	299.0882	9.14	8.87	8-O-Methylretusin	$C_{17}H_{14}O_5$	298.0841	Flavonoid
117	686.3632	9.40	12.70	Avadharidine	$C_{36}H_{51}N_3O_{10}$	685.3574	Alkaloid
118	389.0989	9.95	1.76	Betanidin	$C_{18}H_{16}N_2O_8$	388.0907	Alkaloid
119	345.1958	10.06	8.27	Neotussilagolactone	$C_{21}H_{28}O_4$	344.1988	terpene lactone
120	322.3116 (M+NH4+)	10.28	11.72	3-Pentadecylphenol	$C_{21}H_{36}O$	304.2766	Phenolic
121	391.2586	10.95	18.16	Tussilagone	$C_{23}H_{34}O_5$	390.2406	Phyto
122	610.1535	11.30	21.23	3-Ferulylpelargonidin 5-glucoside	$C_{31}H_{29}O_{13}$	609.1608	Flavonoid
123	699.3237 (M+Na+)	11.29	3.01	Cucurbitacin I 2-glucoside	$C_{36}H_{52}O_{12}$	676.3459	Triterpenoid glycosides
124	561.5062	11.42	6.93	Phytoene 1,2-epoxide	$C_{40}H_{64}O$	560.4957	Sesquaterpenoids
125	531.3789	11.46	11.09	Acinospesigenin A	$C_{32}H_{50}O_6$	530.3607	Triterpenoid

3.3.3. α-amylase and α-glucosidase inhibition activities

Type 2 diabetes is characterized by hyperglycemia and abnormal carbohydrate metabolism. Since it is one of the major causes of morbidity and mortality all over the world, it badly affects the economy worldwide [35]. Several reports are found in literature that describes the plant extracts as potential source to alleviate diabetes and obesity complications through inhibitory effects against α-amylase and α-glucosidase [36–38], however, there is still a continuous need to investigate new plant sources as antidiabetic agents. In continuation of our work on plant extracts, we evaluated different solvent extracts of flowers and leaves of *A. tridactylites* for their α-amylase and α-glucosidase inhibition activities, and the results are presented in Table 3. ATFC and ATLC were the most active against α-amylase with the inhibitory values of 0.61 ± 0.01 and 0.63 ± 0.02 mmol ACAE/g of the extract, respectively, while ATFH and ATLH were second in line with equal inhibitory potential as 0.58 mmol ACAE/g of the extract. In this assay, the ATFA and ATLA were the least active (Table 3) extracts. Against α-glucosidase, ATFH and ATLH exhibited highest inhibitory potential with values of 1.10 ± 0.01 and 1.07 ± 0.01 mmol ACAE/g of the extract, followed by ATFE (1.05 ± 0.05 mmol ACAE/g extract), ATFC (1.04 ± 0.04 mmol ACAE/g extract), ATLC (1.03 ± 0.03 mmol ACAE/g extract) and ATLE (0.94 ± 0.12, Table 3) with minor differences. Literature reports revealed a mixed trend of antidiabetic activities, where sometimes phenolic rich extracts show strong inhibition of amylase [39], while others discloses that low polar solvent fractions show potent amylase inhibition [40]. Another report disclosed the ethyl acetate fractions of plant extracts exhibit better glucosidase inhibition [41], however, this variation could be attributed to different inhibitory assay methods. Overall the extracts of *A. tridactylites* possess significant antidiabetic properties and thus this plant can be a potential source to provide antidiabetic active ingredients.

3.4. Metabolic profiling through UHPLC-MS

The metabolic profiling the ethanolic extract of the whole plant result in identification of 125 compounds (Table 4). Among identified compounds the major classes include phenolic, flavonoids, alkaloids, terpenoids and glycosides. It is believed that phenolic compounds' antioxidant activity is directly related to their chemical structures, such as the number and position of hydroxyl groups. They are good candidates for developing new functional products due to the presence of bioactive compounds as reactive metabolites [42]. Further the presence of terpenoids and triterpenoids glycosides mark this plant important for antioxidant activity [43]. On the other hand, the presence of alkaloids of quinoline and isoquinoline play important role in determining the enzyme activities along terpeionds compounds. Alongside chemical profiling we selected the at least three compounds from major classes phenolic, flavonoids, alkaloids and terpeniods for docking studies. Our findings of enzyme inhibition are supported by docking experiments as well since the docked compounds displayed larger binding free energies than the control.

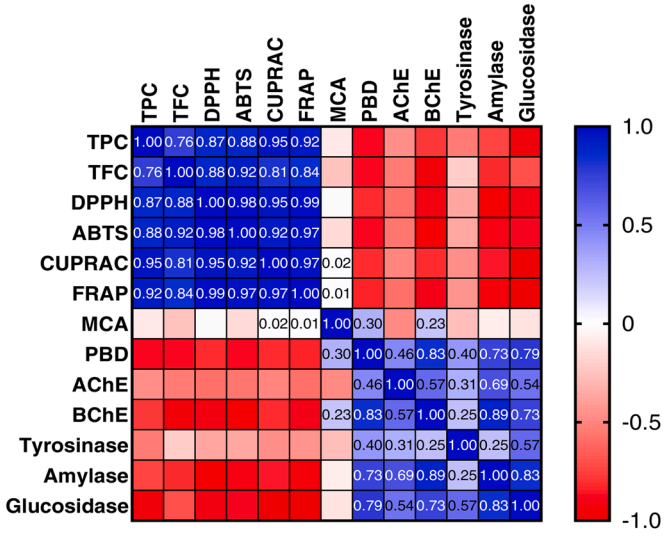

Fig. 1. Pearson correlation values between biological activity assays ($p < 0.05$). TPC: Total phenolic content; TFC: Total flavonoid content; ABTS: 2,2'-azino-bis(3-ethylbenzothiazoline-6-sulfonic acid; DPPH: 1,1-diphenyl-2-picrylhydrazyl; CUPRAC: Cupric reducing antioxidant capacity; FRAP: Ferric reducing antioxidant power; MCA: Metal chelating ability; PBD: Phosphomolybdenum; AChE: acetylcholinesterase; BChE: butyrylcholinesterase;.

3.5. Data mining

There is a growing interest in using multivariate analysis techniques to investigate the relationships and interactions between samples and assays in phytochemical studies. At this point we performed a multivariate analysis for *A. tridactylites* extracts and biological activity assays. First, we performed a Pearson's correlation analysis to explain the interactions between biological activity assays. The results are summarized in Fig. 1. Clearly, the total phenolic and flavonoid contents of the extracts correlated strongly with free radical scavenging and reducing power abilities. Furthermore, we found a good correlation between radical scavenger and reducing power assays. This fact indicated that similar components were the main players in the assays. Consistent with our findings, several investigators reported a positive correlation between total bioactive compounds and the scavenger and reduction properties [44–46]. Unlike radical scavenger and reducing power assays, phosphomolybdenum and metal chelate assays were not correlated

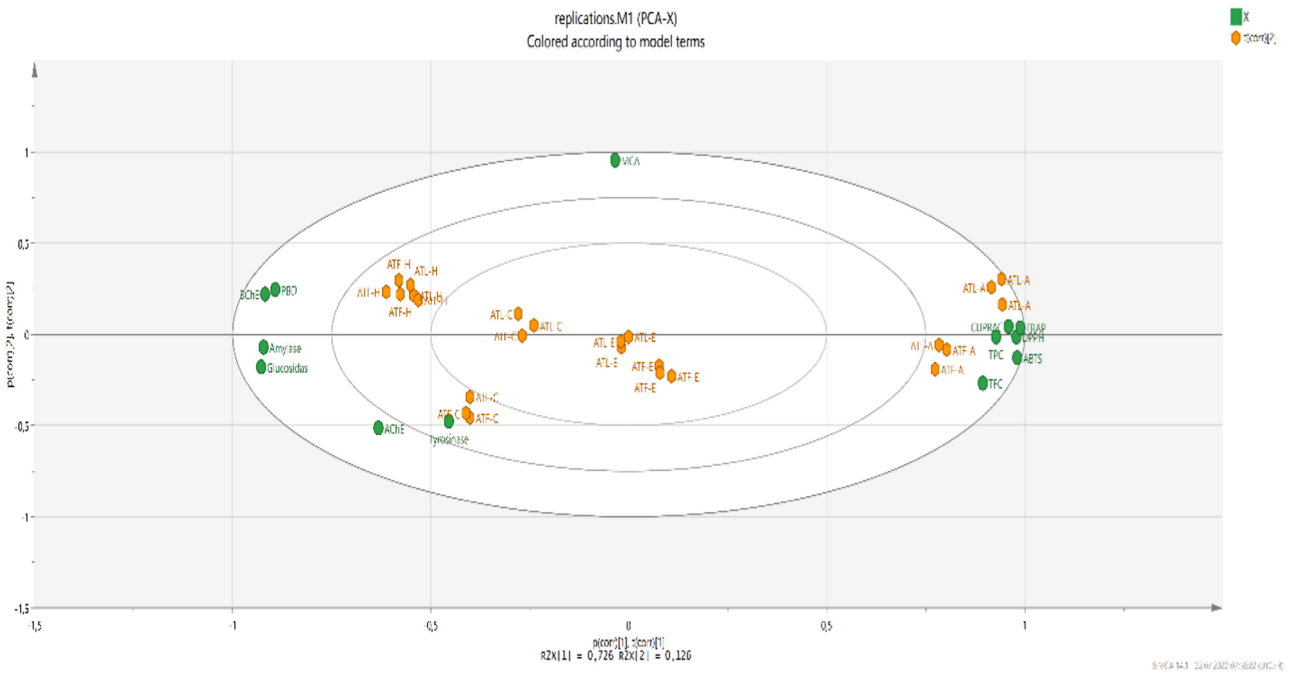

Fig. 2. Biplot graph from principal component analysis between *A. tridactylites* extracts and biological activities.

with total bioactive compounds. This fact could be explained by the presence of non-phenolic antioxidants such as tocopherol or vitamin C. In addition, the metal chelating ability in particular is considered to be a minor factor in the antioxidant mechanisms of phenolics [47]. A principal component analysis was performed on the interactions between the tested extracts. The results are shown in Fig. 2. PCA consisted of two components accounting for 85.2 % of the total components (PC1: 72.6 % and PC2: 12.6). The solvents were clearly distributed differently in the PCA diagram. The ethanol extracts (ATL-A and ATF-A) had the highest levels of total bioactive compounds as well as higher antioxidant properties (radical scavengers and reducing power) and they were very close in the plot. Similar results were also obtained for n-hexane extracts, and their BChE inhibition and phosphomolybdenum abilities were key players in their distribution. Ethyl acetate extracts also had similar effects, particularly on amylase and glucosidase inhibitory properties. In conclusion, we found that the choice of extraction solvents for *A. tridactylites* is one of the most important parameters for the development of new and functional applications utilizing this plant. In this sense, the presented results could be seen as a scientific starting point for large-scale applications.

3.6. Molecular docking analysis

Molecular Docking studies the intermolecular interaction between two molecules in *In-silico*. The protein receptor is the macromolecule in this process. The Ligand molecule, which can serve as an inhibitor, is a micro molecule. The Docking process involves the following steps: The protein's 3D structure should be obtained from the Protein Data Bank (PDB), and then the structure is pre-processed. According to the given parameters, this should allow for the removal of water molecules from the cavity, stability of charges, filling of vacant residues, formation of side chains, and so on. After preparing protein, the active site of protein should be predicted. Although the receptor may have several active sites, just the one that is of concern should be considered. If there are any water molecules or hetero atoms present, they are mostly removed [48, 49]. The ligand be docked against the protein, and the ligand-protein associations are studied. The scoring function specifies a set based on the chosen optimal docked ligand complex. Docking studies of these

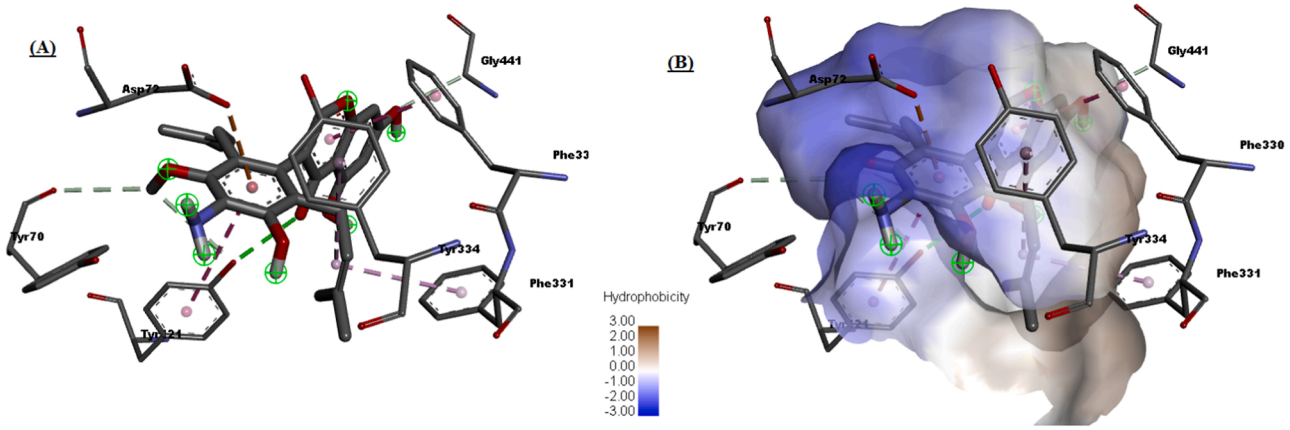

Fig. 3. Molecular docking of compound Piscerythramine with Protein structure for AChE enzyme. (A) 3D view of the best selected conformation: (B) Hydrophobic interactions.

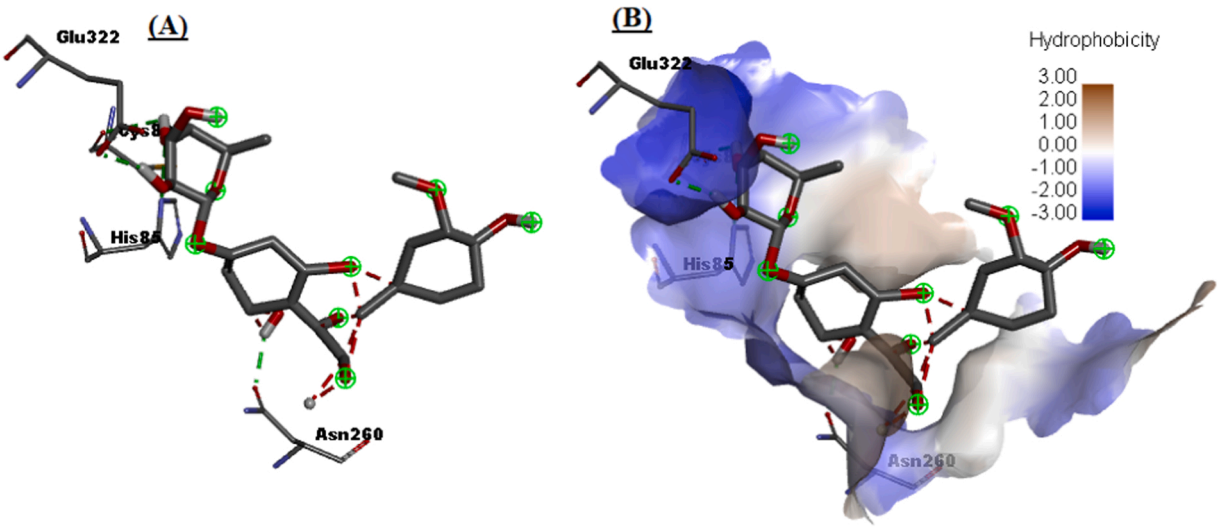

Fig. 4. Molecular docking of compound Isorhamnetin 7-rhamnoside with Protein structure for tyrosinase enzyme. (A) 3D view of the best selected conformation: (B) Hydrophobic interactions.

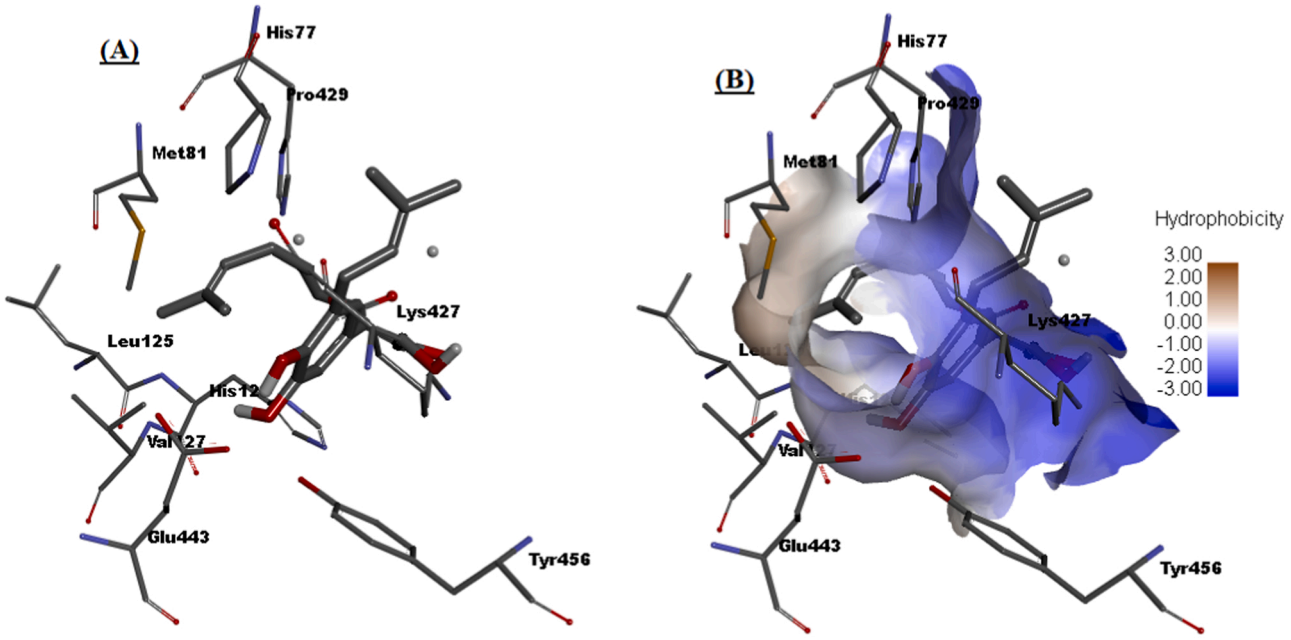

Fig. 5. Molecular docking of compound Isorhamnetin 7-rhamnoside with Protein structure for BChE enzyme. (A) 3D view of the best selected conformation: (B) Hydrophobic interactions.

compounds were performed to determine the binding affinity of these compounds against targeted enzymes. Using Auto Dock software, the binding affinity of these compounds was measured in kcal/mol. For antidiabetic activity we selected two enzymes alpha amylase and alpha glucosidase. Docking of 16 compounds against the targeted enzymes alpha amylase and alpha glucosidase was performed. Docking results for antidiabetic activity against alpha amylase and alpha glucosidase 8 compound showed good binding affinity in the range of − 9.9 to − 8.5 kcal/mol. 16 compound were docked against Tyrosinase inhibitor three compound showed good binding affinity in the range of − 7.0 to − 7.1 kcal/mol. After docking studies out of 16 compound screening, 6 compounds against acetylcholinesterase enzymes showed binding affinity in the range of − 12.3 to − 9.0 kcal/mol, and three compounds against butyrylcholinesterase showed binding affinity in the range of − 6.8–7.5 kcal/mol. Based on their data obtained from docking analysis, the best lead compounds against Ache enzyme were found Piscerythramine with binding affinity − 12.3 KJ/mol with protein (PDB ID: 1EVE) and showing 9 interactions as shown in Fig. 3. For tyrosinase, only three compounds showed good binding affinity and by threshold, one compound Isorhamnetin 7-rhamnoside was found lead compound with highest binding affinity of − 7.1 KJ/mol. It showed 4 interactions with inhibitor protein (PDB ID:2Y9X) as clear from Fig. 4. For BChE enzyme, three compounds showed good results (Table 1). By applying threshold binding affinity as filter, one compound Isorhamnetin 7-rhamnoside with binding affinity − 7.1 KJ/mol. It showed 14 no. of interactions with inhibitor protein (PDB ID: 5nn0) as shown in Fig. 5. Five compounds showed good to excellent inhibition against α-amylase (PDB ID: 3BAJ) and one compound Corchoroside B acting as hit compound with binding affinity of − 9.9 KJ/mol. It showed three interactions as shown in Fig. 6. For α-glucosidase inhibition against protein PDB ID: 3TOP, three compounds showed good results (Table 1) and by applying threshold binding affinity filter, *Sophoradochromene* found a hit

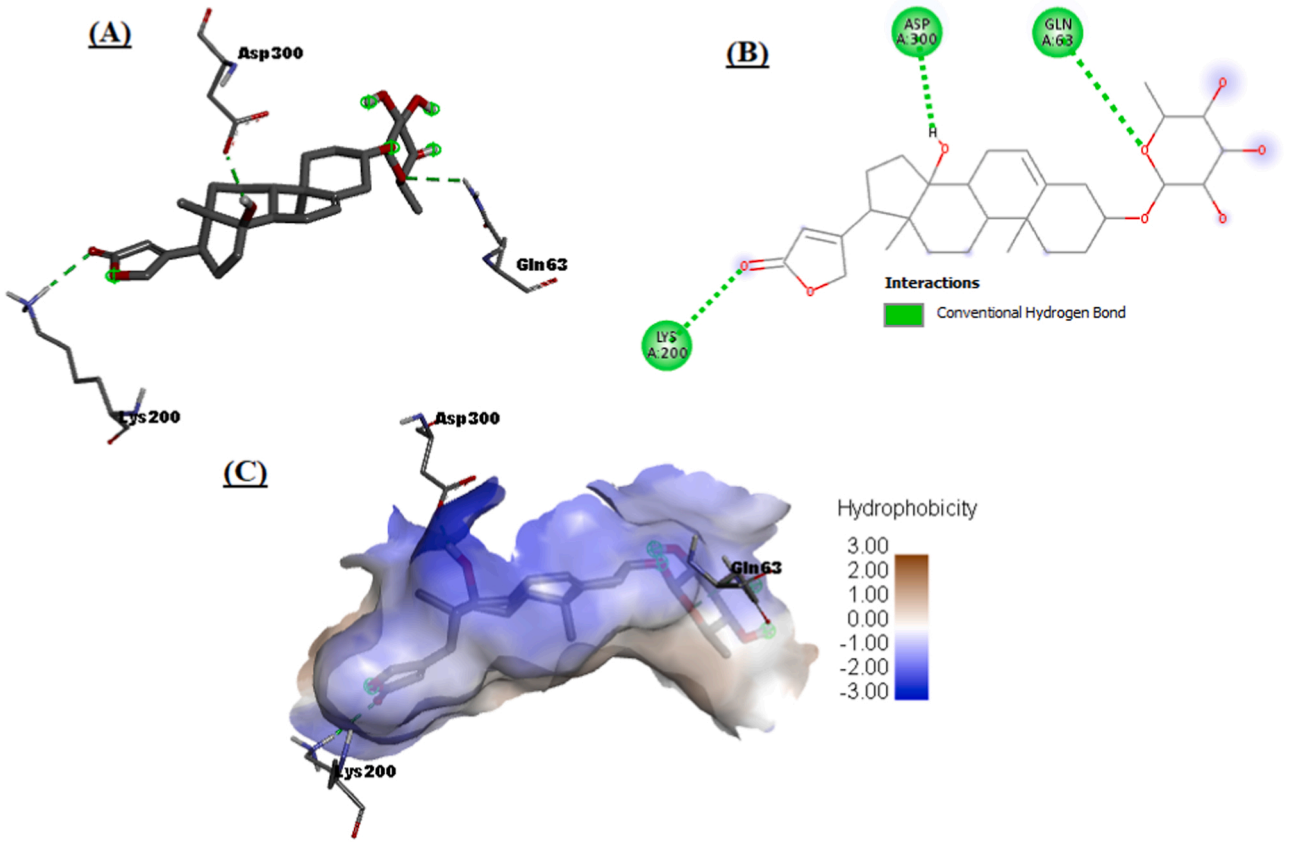

Fig. 6. Molecular docking of compound Corchoroside with Protein structure for α-amylase enzyme. (A) 3D view of the best selected conformation: (B) Hydrophobic interactions.

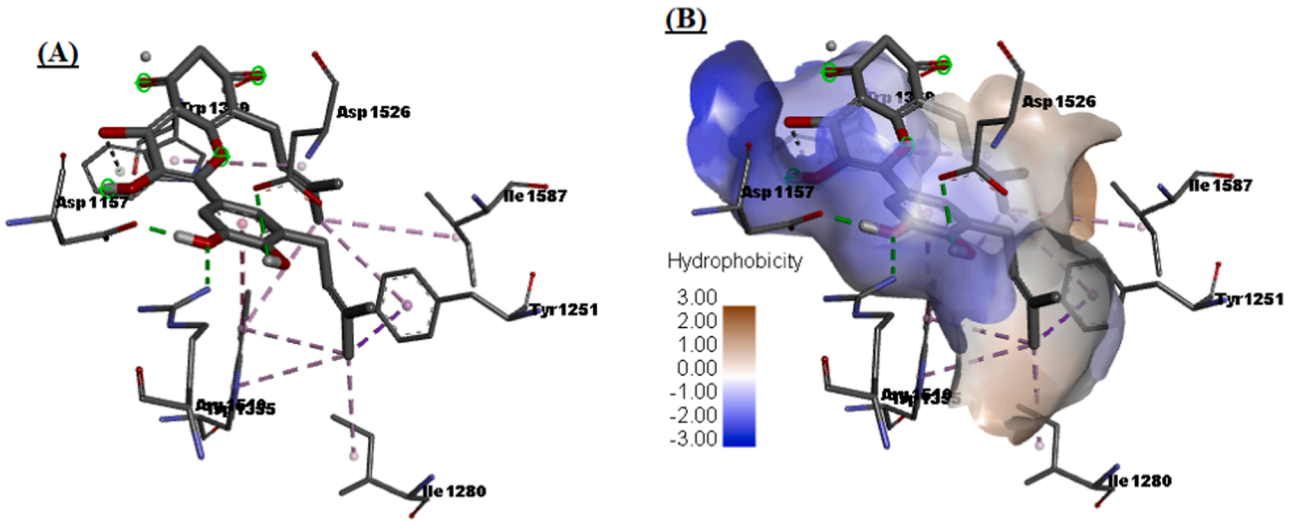

Fig. 7. Molecular docking of compound Sophoradochromene with protein structure for α-glucosidase. A) 3D view of the best selected conformation: B) Hydrophobic interactions.

compound with binding affinity of − 9.3 KJ/mol. It showed thirteen interactions as shown in Fig. 7.(Table. 5).

4. Conclusion

A. tridactylites is locally used against food poisoning; however, scientifically it is totally un-explored herb. The present study leads to conclude that ethanol extract of its flowers and stem are rich in phenolics and flavonoids, while chloroform and ethyl acetate extracts of flowers and stem showed nearly equal phenolic and flavonoid contents but lower than ethanol extract. Further, ethanol fraction of flowers and stem exhibit highest free radical scavenging against DPPH and ABTS, and also was highly active in CUPRA and FRAP assays; these results helped to conclude that mostly phenolics and flavonoids are responsible for antioxidant activity of *A. tridactylites*. On the other hand, hexane extract of both the flowers and the stem showed higher total antioxidant

Table 5
molecular docking interactions and binding affinity of target molecules.

ACHE enzyme							
Compound	Protein	No. of interactions	Amino acid	Distance	Category	Type	*Binding affinity*
Ancistrocladine	*1EVE*	*1*	*PHE331*	*3.37303*	*Hydrogen Bond*	*Carbon Hydrogen*	*-10.1*
		2	*TYR334*	*4.09287*	*Hydrogen Bond*	*Pi-Donor Hydrogen*	
		3	*PHE331*	*3.41279*	*Hydrophobic*	*Pi-Sigma*	
		4	*PHE331*	*5.30779*	*Hydrophobic*	*Pi-Pi Stacked*	
		5	*TYR334*	*4.27734*	*Hydrophobic*	*Pi-Pi Stacked*	
		6	*ILE287*	*4.33704*	*Hydrophobic*	*Alkyl*	
		7	*TYR70*	*5.46811*	*Hydrophobic*	*Pi-Alkyl*	
		8	*TYR121*	*5.37425*	*Hydrophobic*	*Pi-Alkyl*	
		9	*TRP279*	*4.65168*	*Hydrophobic*	*Pi-Alkyl*	
		10	*PHE331*	*5.30647*	*Hydrophobic*	*Pi-Alkyl*	
Brosonoul D		*1*	*TYR70*	*3.01785*	*Hydrogen Bond*	*Conventional hydrogen*	*-11.6*
		2	*TYR70*	*3.11957*	*Hydrogen Bond*	*Conventional hydrogen*	
		3	*TYR121*	*2.85319*	*Hydrogen Bond*	*Conventional hydrogen*	
		4	*PHE288*	*3.15216*	*Hydrogen Bond*	*Conventional hydrogen*	
		5	*TYR70*	*2.52058*	*Hydrogen Bond*	*Conventional hydrogen*	
		6	*ASP72*	*3.35736*	*Electrostatic*	*Pi-Anion*	
		7	*TYR121*	*3.53105*	*Hydrogen Bond*	*Pi-Donor Hydrogen*	
		8	*TRP84*	*3.56902*	*Hydrophobic*	*Pi-Sigma*	
		9	*TYR121*	*5.73184*	*Hydrophobic*	*Pi-Pi T-shaped*	
		10	*TRP84*	*4.79236*	*Hydrophobic*	*Pi-Alkyl*	
		11	*PHE330*	*5.24558*	*Hydrophobic*	*Pi-Alkyl*	
		12	*PHE331*	*4.23026*	*Hydrophobic*	*Pi-Alkyl*	
Echitovenine		*1*	*TYR70*	*3.01785*	*Hydrogen Bond*	*Conventional Hydrogen*	*-9.1*
		2	*TYR70*	*3.11957*	*Hydrogen Bond*	*Bond*	
		3	*TYR121*	*2.85319*	*Hydrogen Bond*	*Conventional Hydrogen*	
		4	*PHE288*	*3.15216*	*Hydrogen Bond*	*Bond*	
		5	*TYR70*	*2.52058*	*Hydrogen Bond*	*Conventional Hydrogen*	
		6	*ASP72*	*3.35736*	*Electrostatic*	*Bond*	
		7	*TYR121*	*3.53105*	*Hydrogen Bond*	*Conventional Hydrogen*	
		8	*TRP84*	*3.56902*	*Hydrophobic*	*Bond*	
		9	*TYR121*	*5.73184*	*Hydrophobic*	*Conventional Hydrogen*	
		10	*TRP84*	*4.79236*	*Hydrophobic*	*Bond*	
		11	*PHE330*	*5.24558*	*Hydrophobic*	*Pi-Anion*	
		12	*PHE331*	*4.23026*	*Hydrophobic*	*Pi-Donor Hydrogen Bond* *Pi-Sigma* *Pi-Pi T-shaped* *Pi-Alkyl* *Pi-Alkyl* *Pi-Alkyl*	
Methyl 3,4-dihydroxy-5-prenylbenzoate 3-glucoside		*1*	*SER122*	*2.91387*	*Hydrogen Bond*	*Conventional Hydrogen*	*-9.0*
		2	*SER200*	*2.7008*	*Hydrogen Bond*	*Bond*	
		3	*1:H*	*2.38296*	*Hydrogen Bond*	*Conventional Hydrogen*	
		4	*TRP84*	*3.5126*	*Hydrogen Bond*	*Bond*	
		5	*TYR130*	*3.68378*	*Hydrogen Bond*	*Conventional Hydrogen*	
		6	*ASP72*	*3.45161*	*Electrostatic*	*Bond* *Carbon Hydrogen Bond* *Carbon Hydrogen Bond* *Pi-Anion*	
Piscerythramine		*1*	*TYR121*	*3.17637*	*Hydrogen Bond*	*Conventional Hydrogen*	*-12.3*
		2	*GLY441*	*2.94139*	*Hydrogen Bond*	*Bond*	
		3	*TYR70*	*3.37077*	*Hydrogen Bond*	*Carbon Hydrogen Bond*	
		4	*TYR121*	*3.66025*	*Hydrogen Bond*	*Carbon Hydrogen Bond*	
		5	*ASP72*	*3.37032*	*Electrostatic*	*Carbon Hydrogen Bond*	
		6	*TYR121*	*5.7737*	*Hydrophobic*	*Pi-Anion*	
		7	*PHE330*	*4.44139*	*Hydrophobic*	*Pi-Pi T-shaped*	
		8	*PHE331*	*4.52038*	*Hydrophobic*	*Pi-Pi T-shaped*	
		9	*TYR334*	*5.34497*	*Hydrophobic*	*Pi-Alkyl* *Pi-Alkyl*	
Thapsigargin		*1*	*TYR121*	*3.02376*	*Hydrogen Bond*	*Conventional Hydrogen*	*-10.0*
		2	*TYR334*	*2.46846*	*Hydrogen Bond*	*Bond*	
		3	*PHE330*	*3.36652*	*Hydrophobic*	*Pi-Donor Hydrogen Bond*	
		4	*TYR70*	*4.61584*	*Hydrophobic*	*Pi-Sigma*	
		5	*TRP279*	*4.12474*	*Hydrophobic*	*Pi-Alkyl*	
		6	*HIS440*	*4.51907*	*Hydrophobic*	*Pi-Alkyl* *Pi-Alkyl*	
Tyrosinase							
Brosonoul D	*2Y9X*	*1*	*ARG268*	*3.31969*	*Hydrogen Bond*	*Conventional Hydrogen*	*-7.0*
		2	*HIS263*	*3.82817*	*Hydrophobic*	*Bond*	
		3	*HIS263*	*3.98664*	*Hydrophobic*	*Pi-Sigma*	
		4	*VAL283*	*4.308*	*Hydrophobic*	*Pi-Sigma*	
		5	*ALA286*	*3.79554*	*Hydrophobic*	*Alkyl*	
		6	*VAL283*	*3.97817*	*Hydrophobic*	*Alkyl*	

(*continued on next page*)

Table 5 (*continued*)

ACHE enzyme							
Compound	Protein	No. of interactions	Amino acid	Distance	Category	Type	*Binding affinity*
		7	*PRO284*	*4.57918*	*Hydrophobic*	*Alkyl*	
		8	*HIS61*	*4.6961*	*Hydrophobic*	*Alkyl*	
		9	*HIS259*	*5.48074*	*Hydrophobic*	*Pi-Alkyl*	
		10	*VAL283*	*4.64751*	*Hydrophobic*	*Pi-Alkyl*	
						Pi-Alkyl	
Isorhamnetin 7-rhamnoside		*1*	*HIS 85*	*2.80854*	*Hydrogen Bond*	*Conventional Hydrogen*	*-7.1*
		2	*GLU322*	*2.09433*	*Hydrogen Bond*	*Bond*	
		3	*CIS83*	*3.05522*	*Hydrogen Bond*	*Conventional Hydrogen*	
		4	*ASN260*	*2.03126*	*Hydrogen Bond*	*Bond*	
						Conventional Hydrogen	
						Bond	
						Conventional Hydrogen	
						Bond	
Methyl 3,4-dihydroxy-5-prenylbenzoate 3-glucoside		*1*	*ARG286*	*3.30816*	*Hydrogen Bond*	*Conventional Hydrogen*	*-7.0*
		2	*VAL283*	*3.20115*	*Hydrogen Bond*	*Bond*	
		3	*VAL283*	*3.33844*	*Hydrogen Bond*	*Conventional Hydrogen*	
		4	*1:H*	*2.38061*	*Hydrogen Bond*	*Bond*	
		5	*SER282*	*3.42707*	*Hydrogen Bond*	*Conventional Hydrogen*	
		6	*HIS244*	*3.65464*	*Hydrogen Bond*	*Bond*	
		7	*HIS263*	*3.61976*	*Hydrophobic*	*Conventional Hydrogen*	
		8	*VAL263*	*4.2981*	*Hydrophobic*	*Bond*	
		9	*HIS61*	*4.71409*	*Hydrophobic*	*Carbon Hydrogen Bond*	
		10	*HIS85*	*4.23444*	*Hydrophobic*	*Carbon Hydrogen Bond*	
		11	*HIS259*	*4.77339*	*Hydrophobic*	*Pi-Sigma*	
		12	*HIS263*	*4.32373*	*Hydrophobic*	*Alkyl*	
		13	*VAL283*	*4.91238*	*Hydrophobic*	*Pi-Alkyl*	
						Pi-Alkyl	
						Pi-Alkyl	
						Pi-Alkyl	
						Pi-Alkyl	
Butyrylcholinesterase							
Brosonoul D	*5nn0*	*1*	*TYR456*	*2.81007*	*Hydrogen Bond*	*Conventional Hydrogenn*	*-6.8*
		2	*GLU443*	*2.37426*	*Hydrogen Bond*	*Conventional Hydrogen*	
		3	*TYR456*	*2.63161*	*Hydrogen Bond*	*Conventional Hydrogen*	
		4	*LYS427*	*3.94187*	*Hydrogen Bond*	*Pi-Cation Hydrogen*	
		5	*HIS126*	*3.88227*	*Hydrophobic*	*Pi-Pi Stacked*	
		6	*MET81*	*4.5082*	*Hydrophobic*	*Alkyl*	
		7	*PRO429*	*3.83427*	*Hydrophobic*	*Alkyl*	
		8	*MET81*	*4.41613*	*Hydrophobic*	*Alkyl*	
		9	*LEU125*	*4.76122*	*Hydrophobic*	*Alkyl*	
		10	*VAL127*	*3.69254*	*Hydrophobic*	*Alkyl*	
		11	*HIS77*	*4.65866*	*Hydrophobic*	*Pi-Alkyl*	
		12	*HIS77*	*4.61532*	*Hydrophobic*	*Pi-Alkyl*	
		13	*HIS126*	*5.0252*	*Hydrophobic*	*Pi-Alkyl*	
		14	*LYS427*	*5.21536*	*Hydrophobic*	*Pi-Alkyl*	
Isorhamnetin 7-rhamnoside		*1*	*TYR456*	*2.81007*	*Hydrogen Bond*	*Conventional hydrogen*	*-7.5*
		2	*GLU443*	*2.37426*	*Hydrogen Bond*	*Conventional hydrogen*	
		3	*TYR456*	*2.63161*	*Hydrogen Bond*	*Conventional hydrogen*	
		4	*LYS427*	*3.94187*	*Hydrogen Bond*	*Pi-Cation;Pi-Donor*	
		5	*HIS126*	*3.88227*	*Hydrophobic*	*Pi-Pi Stacked*	
		6	*MET81*	*4.5082*	*Hydrophobic*	*Alkyl*	
		7	*PRO429*	*3.83427*	*Hydrophobic*	*Alkyl*	
		8	*MET81*	*4.41613*	*Hydrophobic*	*Alkyl*	
		9	*LEU125*	*4.76122*	*Hydrophobic*	*Alkyl*	
		10	*VAL127*	*3.69254*	*Hydrophobic*	*Alkyl*	
		11	*HIS77*	*4.65866*	*Hydrophobic*	*Pi-Alkyl*	
		12	*HIS77*	*4.61532*	*Hydrophobic*	*Pi-Alkyl*	
		13	*HIS126*	*5.0252*	*Hydrophobic*	*Pi-Alkyl*	
		14	*LYS427*	*5.21536*	*Hydrophobic*	*Pi-Alkyl*	
Sophoradochromene		*1*	*HIS177*	*3.09522*	*Hydrogen Bond*	*Conventional Hydrogen*	*-7.3*
		2	*HIS126*	*2.95534*	*Hydrogen Bond*	*Bond*	
		3	*HIS126*	*3.09139*	*Hydrogen Bond*	*Conventional Hydrogen*	
		4	*TYR456*	*2.65649*	*Hydrogen Bond*	*Bond*	
		5	*LEU125*	*3.07246*	*Hydrogen Bond*	*Conventional Hydrogen*	
		6	*HIS77*	*3.55599*	*Hydrogen Bond*	*Bond*	
		7	*HIS77*	*5.25532*	*Hydrophobic*	*Conventional Hydrogen*	
						Bond	
						Carbon Hydrogen Bond	
						Carbon Hydrogen Bond	
						Pi-Alkyl	
α-amylase							
Acinospesigenin A	*3BAJ*	*1*	*TRP59*	*3.82684*	*Hydrophobic*	*Pi-Sigma*	*-8.6*

(*continued on next page*)

Table 5 (*continued*)

ACHE enzyme							
Compound	Protein	No. of interactions	Amino acid	Distance	Category	Type	*Binding affinity*
Ancistrocladine		*1*	*GLN63*	*2.25821*	*Hydrogen Bond*	*Conventional Hydrogen*	*-8.7*
		2	*THR163*	*2.39139*	*Hydrogen Bond*	*Bond*	
		3	*ASP197*	*3.162*	*Hydrogen Bond*	*Conventional Hydrogen*	
		4	*GLU233*	*3.54819*	*Hydrogen Bond*	*Bond*	
		5	*GLU233*	*3.42394*	*Hydrogen Bond*	*Carbon Hydrogen Bond*	
		6	*TRP59*	*4.13814*	*Hydrogen Bond*	*Carbon Hydrogen Bond*	
		7	*TYR62*	*3.8022*	*Hydrophobic*	*Carbon Hydrogen Bond*	
		8	*ALA198*	*4.49694*	*Hydrophobic*	*Pi-Donor Hydrogen Bond*	
		9	*HIS299*	*4.15186*	*Hydrophobic*	*Pi-Sigma*	
		10	*HIS305*	*4.46007*	*Hydrophobic*	*Alkyl*	
		11	*LEU162*	*5.10889*	*Hydrophobic*	*Pi-Alkyl*	
						Pi-Alkyl	
						Pi-Alkyl	
Corchoroside B		*1*	*GLN63*	*2.89337*	*Hydrogen Bond*	*Conventional Hydrogen*	*-9.9*
		2	*LYS200*	*2.44661*	*Hydrogen Bond*	*Bond*	
		3	*ASP300*	*2.07412*	*Hydrogen Bond*	*Conventional Hydrogen*	
						Bond	
						Conventional Hydrogen	
						Bond	
Sophoradochromene		*1*	*GLN63*	*2.78076*	*Hydrogen Bond*	*Conventional Hydrogen*	*-9.7*
		2	*TYR62*	*3.57299*	*Hydrophobic*	*Bond*	
		3	*ALA198*	*3.79781*	*Hydrophobic*	*Pi-Sigma*	
		4	*ILE235*	*4.52239*	*Hydrophobic*	*Alkyl*	
		5	*LYS200*	*4.87512*	*Hydrophobic*	*Alkyl*	
		6	*TRP58*	*5.40942*	*Hydrophobic*	*Alkyl*	
		7	*HIS201*	*5.31149*	*Hydrophobic*	*Pi-Alkyl*	
		8	*HIS201*	*4.32011*	*Hydrophobic*	*Pi-Alkyl*	
		9	*LEU162*	*5.0168*	*Hydrophobic*	*Pi-Alkyl*	
		10	*LEU165*	*5.01377*	*Hydrophobic*	*Pi-Alkyl*	
						Pi-Alkyl	
Spinacoside D		*1*	*HIS305*	*2.46902*	*Hydrogen Bond*	*Conventional Hydrogen*	*-8.9*
		2	*ASP300*	*3.29428*	*Hydrogen Bond*	*Bond*	
		3	*THR163*	*3.39873*	*Hydrogen Bond*	*Carbon Hydrogen Bond*	
		4	*TRP59*	*3.81021*	*Hydrophobic*	*Carbon Hydrogen Bond*	
		5	*TYR151*	*5.64157*	*Hydrophobic*	*Pi-Sigma*	
		6	*ILE235*	*5.15991*	*Hydrophobic*	*Pi-Pi T-shaped*	
		7	*TRP59*	*4.38619*	*Hydrophobic*	*Alkyl*	
						Pi-Alkyl	
α-glucosidase							
Brosonoul D	*3TOP*	*1*	*ARG1510*	*2.5771*	*Hydrogen Bond*	*Conventional Hydrogen*	*-9.1*
		2	*ASP1157*	*1.66717*	*Hydrogen Bond*	*Bond*	
		3	*ASP1526*	*2.59055*	*Hydrogen Bond*	*Conventional Hydrogen*	
		4	*TRP1369*	*4.06277*	*Hydrogen Bond*	*Bond*	
		5	*TYR1251*	*3.64362*	*Hydrophobic*	*Conventional Hydrogen*	
		6	*TRP1355*	*5.1156*	*Hydrophobic*	*Bond*	
		7	*ILE1280*	*4.25889*	*Hydrophobic*	*Pi-Donor Hydrogen Bond*	
		8	*ILE1587*	*5.10069*	*Hydrophobic*	*Pi-Sigma*	
		9	*TYR1251*	*5.00475*	*Hydrophobic*	*Pi-Pi T-shaped*	
		10	*TRP1355*	*4.63907*	*Hydrophobic*	*Alkyl*	
		11	*TRP1355*	*4.65693*	*Hydrophobic*	*Alkyl*	
		12	*TRP1355*	*5.26381*	*Hydrophobic*	*Pi-Alkyl*	
		13	*TRP1369*	*5.44334*	*Hydrophobic*	*Pi-Alkyl*	
						Pi-Alkyl	
						Pi-Alkyl	
						Pi-Alkyl	
Sophoradochromene		*1*	*ARG1510*	*2.5771*	*Hydrogen Bond*	*Conventional Hydrogen*	*-9.3*
		2	*ASP1157*	*1.66717*	*Hydrogen Bond*	*Bond*	
		3	*ASP1526*	*2.59055*	*Hydrogen Bond*	*Conventional Hydrogen*	
		4	*TRP1369*	*4.06277*	*Hydrogen Bond*	*Bond*	
		5	*TYR1251*	*3.64362*	*Hydrophobic*	*Conventional Hydrogen*	
		6	*TRP1355*	*5.1156*	*Hydrophobic*	*Bond*	
		7	*ILE1280*	*4.25889*	*Hydrophobic*	*Pi-Donor Hydrogen Bond*	
		8	*ILE1587*	*5.10069*	*Hydrophobic*	*Pi-Sigma*	
		9	*TYR1251*	*5.00475*	*Hydrophobic*	*Pi-Pi T-shaped*	
		10	*TRP1355*	*4.63907*	*Hydrophobic*	*Alkyl*	
		11	*TRP1355*	*4.65693*	*Hydrophobic*	*Alkyl*	
		12	*TRP1355*	*5.26381*	*Hydrophobic*	*Pi-Alkyl*	
		13	*TRP1369*	*5.44334*	*Hydrophobic*	*Pi-Alkyl*	
						Pi-Alkyl	
						Pi-Alkyl	
						Pi-Alkyl	
Spinacoside D		*1*	*LYS1460*	*3.01899*	*Hydrogen Bond*	*Conventional Hydrogen*	*-9.2*
		2	*LYS1460*	*4.22699*	*Electrostatic*	*Bond*	

(*continued on next page*)

Table 5 (*continued*)

ACHE enzyme							
Compound	Protein	No. of interactions	Amino acid	Distance	Category	Type	*Binding affinity*
		3	*ASP1526*	*4.984*	*Electrostatic*	*Pi-Cation*	
		4	*TYR1251*	*3.66647*	*Hydrophobic*	*Pi-Anion*	
		5	*PHE1560*	*3.84811*	*Hydrophobic*	*Pi-Sigma*	
		6	*TRP1355*	*5.15621*	*Hydrophobic*	*Pi-Sigma*	
		7	*TRP1369*	*5.42213*	*Hydrophobic*	*Pi-Pi T-shaped*	
		8	*TRP1369*	*5.14468*	*Hydrophobic*	*Pi-Pi T-shaped*	
		9	*PHE1559*	*5.62421*	*Hydrophobic*	*Pi-Pi T-shaped*	
		10	*ILE1587*	*5.32555*	*Hydrophobic*	*Pi-Pi T-shaped*	
		11	*TYR1251*	*4.86861*	*Hydrophobic*	*Alkyl*	
		12	*TRP1355*	*5.46378*	*Hydrophobic*	*Pi-Alkyl*	
		13	*TRP1369*	*5.40224*	*Hydrophobic*	*Pi-Alkyl*	
		14	*PHE1560*	*4.09112*	*Hydrophobic*	*Pi-Alkyl*	
						Pi-Alkyl	

capacity, metal chelating and enzyme inhibition activities, which led to concluded that other constituents also impart to medicinal potential of *A. tridactylites*. It is thus finally concluded that *A. tridactylites* is a new and rich source of antioxidant compounds and can be potential component of health promoting formulations.

Data availability

Data will be made available on request.

Acknowledgment

The authors from King Khalid University acknowledge the financial support from Research Center for Advanced Material Science (RCAMS) at King Khalid University through grant number RCAMS/KKU/027–23.

References

[1] A.G. Atanasov, S.B. Zotchev, V.M. Dirsch, C.T. Supuran, Natural products in drug discovery: advances and opportunities, Nat. Rev. Drug Discov. 20 (3) (2021) 200–216.
[2] Z. Abbas, S. Kousar, M.A. Aziz, A. Pieroni, A.A. Aldosari, R.W. Bussmann, G. Raza, A.M. Abbasi, Comparative assessment of medicinal plant utilization among Balti and Shina communities in the periphery of Deosai National Park, Pakistan, Biology 10 (5) (2021) 434.
[3] www.eFloras.org, Allardia tridactylites (Karelin & Kirilov), 2022. http://www.efloras.org/florataxon.aspx?flora_id=2&taxon_id=242101012. (Accessed 01/02/2022 2022).
[4] R.B.G. KEW, Allardia tridactylites (Kar. & Kir.) Sch.Bip., 2022. ⟨https://powo.science.kew.org/taxon/urn:lsid:ipni.org:names:175906–1#distribution-map⟩. (Accessed 01/02/2022 2022).
[5] A. Giorgi, S. Panseri, M.S. Mattara, C. Andreis, L.M. Chiesa, Secondary metabolites and antioxidant capacities of Waldheimia glabra (Decne.) Regel from Nepal, J. Sci. Food Agric. 93 (5) (2013) 1026–1034.
[6] J. De, Y. Lu, L. Ling, N. Peng, Y. Zhong, Essential oil composition and bioactivities of Waldheimia glabra (Asteraceae) from Qinghai-Tibet plateau, Molecules 22 (3) (2017) 460.
[7] A. Manzo, L. Musso, S. Panseri, M. Iriti, S. Dallavalle, E. Catalano, G. Scarì, A. Giorgi, Screening of the chemical composition and bioactivity of Waldheimia glabra (Decne.) Regel essential oil, J. Sci. Food Agric. 96 (9) (2016) 3195–3201.
[8] M. Zubair, M. Nazir, M. Saleem, N. Raiz, S. Touseef, S. Khan, G. Zengin, M. Ehsan Mazhar, M. Imran Tousif, Chemodiversity, biological activities and molecular docking studies of Leptadenia pyrotechnica (Forssk.) Decne: a comprehensive approach to validate its medicinal use, Chem. Biodivers. 19 (5) (2022), e202100884.
[9] M.I. Tousif, M. Nazir, M. Saleem, S. Tauseef, R. Uddin, M. Altaf, G. Zengin, G. Ak, R.B. Ozturk, M.F. Mahomoodally, Exploring the industrial importance of a miracle herb Withania somnifera (L.) Dunal: authentication through chemical profiling, in vitro studies and computational analyses, Process Biochem. 121 (2022) 514–528.
[10] M. Saleem, N. Shazmeen, M. Nazir, N. Riaz, G. Zengin, H.M. Ataullah, F. Nisar, M. Mukhtar, M.I. Tousif, Investigation on the phytochemical composition, antioxidant and enzyme inhibition potential of polygonum plebeium R. Br: a comprehensive approach to disclose new nutraceutical and functional food ingredients, Chem. Biodivers. 18 (12) (2021), e2100706.
[11] N. Shazmeen, M. Nazir, N. Riaz, M. Saleem, M.I. Tousif, S. Tauseef, R. Uddin, M. Mukhtar, G. Zengin, A. Mollica, In vitro antioxidant and enzyme inhibitory studies, computational analysis and chemodiversity of an emergency food plant Caralluma edulis (Edgew.) Benth. ex Hook. f: A multifunctional approach to provide new ingredients for nutraceuticals and functional foods, Food Biosci. 50 (2022), 102097.
[12] G. Luisi, A. Stefanucci, G. Zengin, M.P. Dimmito, A. Mollica, Anti-oxidant and tyrosinase inhibitory in vitro activity of amino acids and small peptides: new hints for the multifaceted treatment of neurologic and metabolic disfunctions, Antioxidants 8 (1) (2018) 7.
[13] M. Saleem, N. Shazmeen, M. Nazir, N. Riaz, G. Zengin, H.M. Ataullah, F. Nisar, M. Mukhtar, M.I. Tousif, Investigation on the phytochemical composition, antioxidant and enzyme inhibition potential of polygonum plebeium R. Br: a comprehensive approach to disclose new nutraceutical and functional food ingredients, Chem. Biodivers. 18 (12) (2021), e2100706.
[14] M.F. Mahomoodally, A. Mollica, A. Stefanucci, M.Z. Aumeeruddy, R. Poorneeka, G. Zengin, Volatile components, pharmacological profile, and computational studies of essential oil from Aegle marmelos (Bael) leaves: a functional approach, Ind. Crops Prod. 126 (2018) 13–21.
[15] S. Khan, M. Nazir, N. Raiz, M. Saleem, G. Zengin, G. Fazal, H. Saleem, M. Mukhtar, M.I. Tousif, R.B. Tareen, Phytochemical profiling, in vitro biological properties and in silico studies on Caragana ambigua stocks (Fabaceae): a comprehensive approach, Ind. Crops Prod. 131 (2019) 117–124.
[16] H.M. Berman, J. Westbrook, Z. Feng, G. Gilliland, T.N. Bhat, H. Weissig, I. N. Shindyalov, P.E. Bourne, The protein data bank, Nucleic Acids Res. 28 (1) (2000) 235–242.
[17] V. Schnecke, L.A. Kuhn, Virtual screening with solvation and ligand-induced complementarity, virtual screening: an alternative or complement to high throughput screening? 2000. pp. 171–190.
[18] D.S.S. Delmondes, P.H. Delmondes, Molecular docking study of phenolic compounds with chitosan: planning of biodegradable hydrogels with antioxidant action. Proceedings of MOL2NET 2018, International Conference on Multidisciplinary Sciences, Fourth ed., MDPI, 2018, p. 1.
[19] O. Trott, A.J. Olson, AutoDock Vina: improving the speed and accuracy of docking with a new scoring function, efficient optimization, and multithreading, J. Comput. Chem. 31 (2) (2010) 455–461.
[20] P.H. Delmondes, R. Stefani, Molecular docking studies of natural phenolic compound and derivates with phospholipase A2, Orbit.: Electron. J. Chem. 10 (6) (2018) 467–474.
[21] E. Tejera, C.R. Munteanu, A. López-Cortés, A. Cabrera-Andrade, Y. Pérez-Castillo, Drugs repurposing using QSAR, docking and molecular dynamics for possible inhibitors of the SARS-CoV-2 Mpro protease, Molecules 25 (21) (2020) 5172.
[22] K. Dileep, I. Tintu, C. Sadasivan, Molecular docking studies of curcumin analogs with phospholipase A2, Interdiscip. Sci. Comput. Life Sci. 3 (3) (2011) 189–197.
[23] R. Herowati, G.P. Widodo, Molecular docking analysis: interaction studies of natural compounds to anti-inflammatory targets, QSAR (2017) 63.
[24] A.M. Hassan, A.M. Dhumad, R. Al-Asadi, A.M. Jassem, Synthesis and molecular docking of some amic acid targeting breast cancer. IOP Conference Series: Materials Science and Engineering, IOP Publishing, 2020.
[25] S.M. Sadati, N. Gheibi, S. Ranjbar, M.S. Hashemzadeh, Docking study of flavonoid derivatives as potent inhibitors of influenza H1N1 virus neuraminidase, Biomed. Rep. 10 (1) (2019) 33–38.
[26] N. Saeed, M.R. Khan, M. Shabbir, Antioxidant activity, total phenolic and total flavonoid contents of whole plant extracts Torilis leptophylla L, BMC Complement. Altern. Med. 12 (2012) 1–12.
[27] T. Tomova, V. Petkov, I. Slavova, P. Stoyanov, M. Argirova, Naturally present metal ions in plants could interfere with common antioxidant assays, MethodsX 7 (2020), 100995.
[28] R. Sudan, M. Bhagat, S. Gupta, J. Singh, A. Koul, Iron (FeII) chelation, ferric reducing antioxidant power, and immune modulating potential of Arisaema jacquemontii (Himalayan Cobra Lily), BioMed. Res. Int. 2014 (2014), 179865.
[29] M. Rosillo-Lopez, C.G. Salzmann, Highly efficient heavy-metal extraction from water with carboxylated graphene nanoflakes, RSC Adv. 8 (20) (2018) 11043–11050.
[30] S.J. Flora, V. Pachauri, Chelation in metal intoxication, Int. J. Environ. Res. Public Health 7 (7) (2010) 2745–2788.
[31] Y.-R. Zhang, Y.-Z. Huang, Q.-L. Bao, X.-D. Wei, B.-Q. Tie, S.-N. Zhang, N. Han, Y.-C. Huang, Effect of chelating agents and organic acids on remediation of cadmium

and arsenic complex contaminated soil using Xanthium sibiricum, Huan Jing ke Xue=, Huanjing Kexue 43 (8) (2022) 4292–4300.
[32] T.-S. Chang, An updated review of tyrosinase inhibitors, Int. J. Mol. Sci. 10 (6) (2009) 2440–2475.
[33] A. Di Petrillo, A. María González-Paramás, A. Rosa, V. Ruggiero, F. Boylan, A. Kumar, F. Pintus, C. Santos-Buelga, A. Fais, B. Era, Chemical composition and enzyme inhibition of Phytolacca dioica L. seeds extracts, J. Enzym. Inhib. Med. Chem. 34 (1) (2019) 519–527.
[34] Y. Haliloglu, T. Ozek, M. Tekin, F. Goger, K.H.C. Baser, G. Ozek, Phytochemicals, antioxidant, and antityrosinase activities of Achillea sivasica Çelik and Akpulat, Int. J. Food Prop. 20 (sup1) (2017) S693–S706.
[35] J. Upadhyay, S.A. Polyzos, N. Perakakis, B. Thakkar, S.A. Paschou, N. Katsiki, P. Underwood, K.-H. Park, J. Seufert, E.S. Kang, Pharmacotherapy of type 2 diabetes: an update, Metabolism 78 (2018) 13–42.
[36] T. Buchholz, M.F. Melzig, Medicinal plants traditionally used for treatment of obesity and diabetes mellitus–screening for pancreatic lipase and α-Amylase inhibition, Phytother. Res. 30 (2) (2016) 260–266.
[37] H. Rupasinghe, N. Balasuriya, Y. Wang, Prevention of type 2 diabetes by polyphenols of fruits. Nutritional Antioxidant Therapies: Treatments and Perspectives, Springer, 2017, pp. 447–466.
[38] S. Sekhon-Loodu, H.V. Rupasinghe, Evaluation of antioxidant, antidiabetic and antiobesity potential of selected traditional medicinal plants, Front. Nutr. 6 (2019) 53.
[39] V.T.T. Anh, D.T.X. Trang, K. Kamei, T.C. Linh, N.H. Pham-Khanh, N.T. Tuan, L. T. Danh, Phytochemicals, antioxidant and antidiabetic activities of extracts from Miliusa velutina flowers, Horticulturae 7 (12) (2021) 555.
[40] N.M. Alema, G. Periasamy, G.G. Sibhat, G.H. Tekulu, M.G. Hiben, Antidiabetic activity of extracts of Terminalia brownii Fresen. Stem bark in mice, J. Exp. Pharmacol. 12 (2020) 61.
[41] A. Bhatia, B. Singh, R. Arora, S. Arora, In vitro evaluation of the α-glucosidase inhibitory potential of methanolic extracts of traditionally used antidiabetic plants, BMC Complement. Altern. Med. 19 (1) (2019) 1–9.
[42] Y. Aguilera, I. Estrella, V. Benitez, R.M. Esteban, M.A. Martín-Cabrejas, Bioactive phenolic compounds and functional properties of dehydrated bean flours, Food Res. Int. 44 (3) (2011) 774–780.
[43] Y.S. Kil, S.M. Sin, D.Y. Lee, W.M. Jeong, S.-W. Lee, Y.-H. Kim, Y.-M. Goo, Analysis of triterpene glycoside levels and antioxidant activity in the different shoot tissues of Centella asiatica (L.) Urban, J. Life Sci. 28 (8) (2018) 917–922.
[44] A. ben Jalloul, H. Chaar, M.S. Tounsi, M. Abderrabba, Variations in phenolic composition and antioxidant activities of Scabiosa maritima (Scabiosa atropurpurea sub. maritima L.) crude extracts and fractions according to growth stage and plant part, South Afr. J. Bot. 146 (2022) 703–714.
[45] S. Salman, G. Öz, R. Felek, A. Haznedar, T. Turna, F. Özdemir, Effects of fermentation time on phenolic composition, antioxidant and antimicrobial activities of green, oolong, and black teas, Food, Bioscience 49 (2022), 101884.
[46] J. Wei, T. Su, H. Su, Y. Jiang, J. Li, Y. Bi, Comparative assessment of phenolics, antioxidant and antiproliferative activities between Hippophae rhamnoides ssp. sinensis and H. tibetana leaf in Qinghai-Tibet Plateau, Food Biosci. 46 (2022), 101507.
[47] C. Rice-Evans, N. Miller, G. Paganga, Antioxidant properties of phenolic compounds, Trends Plant Sci. 2 (4) (1997) 152–159.
[48] C. Mcmartin, R.S. Bohacek, QXP: powerful, rapid computer algorithms for structure-based drug design, J. Comput. Aided Mol. Des. 11 (4) (1997) 333–344.
[49] V. Schnecke, L.A. Kuhn, Virtual screening with solvation and ligand-induced complementarity. Virtual Screening: An Alternative or Complement to High Throughput Screening?, Springer, 2000, pp. 171–190.